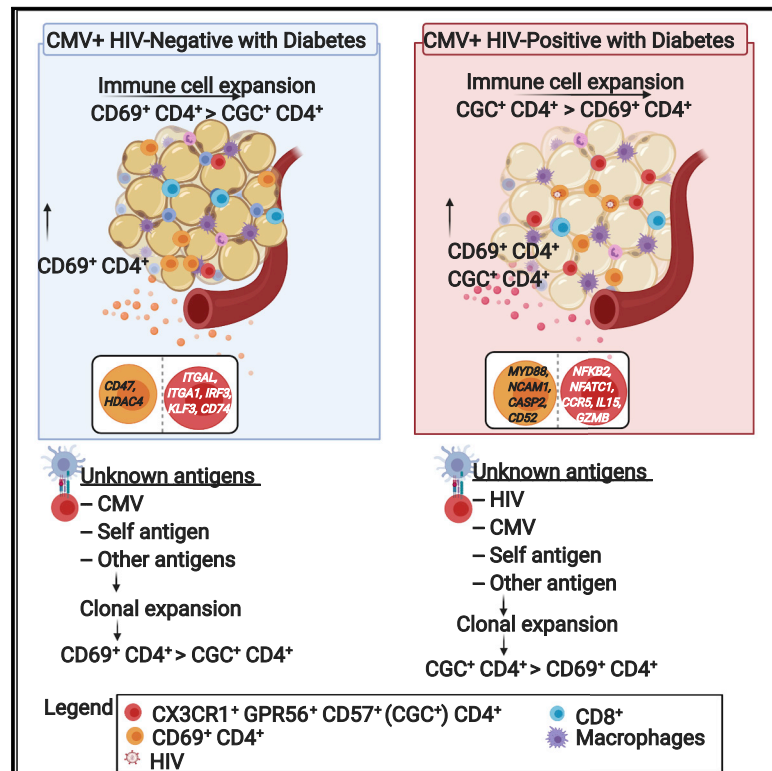**Article**

Single-cell analysis shows that adipose tissue of persons with both HIV and diabetes is enriched for clonal, cytotoxic, and CMV-specific CD4+ T cells

Graphical Abstract

Highlights

- Adipose tissue memory CD4$^+$ T cells are frequently CD69$^+$ in persons with diabetes

- Persons with HIV and diabetes have more CX3CR1$^+$ GPR56$^+$ CD57$^+$ (C-G-C$^+$) CD4$^+$ T cells

- Adipose tissue C-G-C$^+$ CD4$^+$ T cells and CD69$^+$ CD4$^+$ T cells are clonally expanded

- C-G-C$^+$ CD4$^+$ T cells are often CMV specific and have more inflammatory transcriptomes

Authors

Celestine N. Wanjalla,
Wyatt J. McDonnell, Ramesh Ram, ...,
Simon A. Mallal, Spyros A. Kalams,
John R. Koethe

Correspondence

celestine.wanjalla@vumc.org (C.N.W.),
john.r.koethe@vumc.org (J.R.K.)

In Brief

Wanjalla et al. demonstrate that adipose tissue in persons with HIV and diabetes includes a large proportion of clonally expanded, inflammatory, and frequently CMV-specific CX3CR1$^+$ GPR56$^+$ CD57$^+$ (C-G-C$^+$) CD4$^+$ T cells. These cells may contribute to the altered adipocyte function and elevated risk of metabolic disease observed among persons with HIV.

CellPress

Article

Single-cell analysis shows that adipose tissue of persons with both HIV and diabetes is enriched for clonal, cytotoxic, and CMV-specific CD4+ T cells

Celestine N. Wanjalla,[1,2,5,14,*] Wyatt J. McDonnell,[1,2,3,4,11] Ramesh Ram,[10] Abha Chopra,[10] Rama Gangula,[1,5] Shay Leary,[10] Mona Mashayekhi,[6] Joshua D. Simmons,[1,5] Christian M. Warren,[1,5] Samuel Bailin,[1] Curtis L. Gabriel,[8] Liang Guo,[12] Briana D. Furch,[1,5] Morgan C. Lima,[1,5] Beverly O. Woodward,[1,5] LaToya Hannah,[6] Mark A. Pilkinton,[1,2] Daniela T. Fuller,[12] Kenji Kawai,[12] Renu Virmani,[12] Aloke V. Finn,[12] Alyssa H. Hasty,[9,13] Simon A. Mallal,[1,2,4,5,7,10] Spyros A. Kalams,[1,2,4,5] and John R. Koethe[1,2,5,13,15,*]

[1]Division of Infectious Diseases, Department of Medicine, Vanderbilt University Medical Center, Nashville, TN, USA
[2]Center for Translational Immunology and Infectious Disease, Vanderbilt University Medical Center, Nashville, TN, USA
[3]Vanderbilt Vaccine Center, Vanderbilt University Medical Center, Nashville, TN, USA
[4]Department of Pathology, Microbiology, and Immunology, Vanderbilt University, Nashville, TN, USA
[5]Tennessee Center for AIDS Research, Vanderbilt University Medical Center, Nashville, TN, USA
[6]Division of Diabetes, Endocrinology and Metabolism, Vanderbilt University Medical Center, Nashville, TN, USA
[7]VANTAGE, Vanderbilt University Medical Center, Nashville, TN, USA
[8]Division of Gastroenterology, Hepatology and Nutrition, Vanderbilt University, Nashville, TN, USA
[9]Department of Molecular Physiology and Biophysics, Vanderbilt University, Nashville, TN, USA
[10]Institute for Immunology and Infectious Diseases, Murdoch University, Perth, WA, Australia
[11]10x Genomics, Pleasanton, CA, USA
[12]CVPath Institute, Gaithersburg, MD, USA
[13]Veterans Affairs Tennessee Valley Healthcare System, Nashville, TN, USA
[14]Twitter: @CWanjallaMDPhD
[15]Lead contact
*Correspondence: celestine.wanjalla@vumc.org (C.N.W.), john.r.koethe@vumc.org (J.R.K.)
https://doi.org/10.1016/j.xcrm.2021.100205

SUMMARY

Persons with HIV are at increased risk for diabetes mellitus compared with individuals without HIV. Adipose tissue is an important regulator of glucose and lipid metabolism, and adipose tissue T cells modulate local inflammatory responses and, by extension, adipocyte function. Persons with HIV and diabetes have a high proportion of CX3CR1$^+$ GPR56$^+$ CD57$^+$ (C-G-C$^+$) CD4$^+$ T cells in adipose tissue, a subset of which are cytomegalovirus specific, whereas individuals with diabetes but without HIV have predominantly CD69$^+$ CD4$^+$ T cells. Adipose tissue CD69$^+$ and C-G-C$^+$ CD4$^+$ T cell subsets demonstrate higher receptor clonality compared with the same cells in blood, potentially reflecting antigen-driven expansion, but C-G-C$^+$ CD4$^+$ T cells have a more inflammatory and cytotoxic RNA transcriptome. Future studies will explore whether viral antigens have a role in recruitment and proliferation of pro-inflammatory C-G-C$^+$ CD4$^+$ T cells in adipose tissue of persons with HIV.

INTRODUCTION

Adipose tissue contains a diverse array of innate and adaptive immune cells that defend against pathogens, aid removal of apoptotic cellular debris, and modulate adipocyte homeostasis and energy utilization.[1] Human immunodeficiency virus (HIV) establishes a latent pro-viral presence in multiple tissue compartments, including adipose tissue. This is accompanied by profound shifts in the relative proportions of adipose tissue CD4$^+$ and CD8$^+$ T cells, immune cell surface marker phenotypes, antigen receptor repertoire, adipocyte gene expression, and energy homeostasis.[2–7]

Persons with HIV can now survive decades on effective antiretroviral therapy, but this success is offset by a rising burden of metabolic diseases.[8–10] The altered innate and adaptive immune

environment in adipose tissue of HIV-positive persons raises the question of whether these immune cells contribute to metabolic dysregulation, as observed in obesity. In obesity, progressive weight gain is accompanied by recruitment of activated M1-like pro-inflammatory macrophages into adipose tissue along with infiltration of CD8$^+$ T cells, a shift from anti-inflammatory T$_H$2 to pro-inflammatory T$_H$1 CD4$^+$ cells, reduced regulatory T cells, increased local inflammatory cytokines, and reduced glucose tolerance.[11–14] Although HIV and obesity are both characterized by an increase in the ratio of adipose tissue CD8$^+$ to CD4$^+$ T cells,[11,12,15] our group has shown recently that differences in adipose tissue CD4$^+$ T cell populations, as opposed to CD8$^+$ T cells, are a defining feature of metabolic disease in HIV-positive persons. We found that the phenotype of adipose CD8$^+$ T cell subsets (naive, central memory [T$_{CM}$], effector

memory [T_{EM}], and effector memory CD45RA$^+$ [T_{EMRA}] cells) was similar irrespective of metabolic health. However, adipose tissue from HIV-positive diabetics was enriched significantly in several distinct CD4$^+$ T cell subsets compared with HIV-positive non-diabetics: CD69$^+$ T_{EM} cells and CD69$^-$ CX3CR1$^+$ GPR56$^+$ CD57$^+$ T_{EM} and T_{EMRA} cells.[7]

The finding of greater CX3CR1, GPR56, and CD57 co-expression (hereafter referred to as C-G-C co-expression) on CD4$^+$ T_{EM} and T_{EMRA} cells in adipose tissue from HIV-positive diabetics was notable because this marker combination may reflect anti-viral activity. Virus-specific T_{EMRA} cells are more frequently GPR56$^+$,[16] and increased expression of GPR56 and killer-like receptors (KLRs) has been linked to higher CD4$^+$ T cell cytokine expression.[17] Furthermore, cytotoxic GPR56$^+$ CD4$^+$ and CD8$^+$ T_{EMRA} cells have higher co-expression of the CX3CR1 receptor,[16,18,19] which is also a marker of anti-cytomegalovirus (CMV) T cells.[19–22] Given that adipose tissue serves as a reservoir for latently HIV-infected CD4$^+$ T cells, free HIV RNA virus, and CMV,[2,3,6,23] greater C-G-C$^+$ co-expression on CD4$^+$ T cells in adipose tissue of HIV-positive diabetics may reflect a cytotoxic response by virus-specific cells that adversely affects bystander adipocytes and contributes to metabolic disease.[24–26]

In this study, we used multiparameter indexed flow cytometry, bulk T cell receptor (TCR) sequencing and single-cell RNA sequencing (scRNA-seq) to profile adipose tissue CD4$^+$ T cells in HIV-positive non-diabetics, diabetics, and a control group of HIV-negative diabetics. We hypothesized that latent pro-viral HIV/replicating HIV and other viruses, such as CMV, present in subcutaneous adipose tissue promote recruitment and expansion of pro-inflammatory and cytotoxic virus-specific CD4$^+$ T cells, which may contribute to development of glucose intolerance. Here we report that a larger proportion of total CD4$^+$ T cells co-express the C-G-C surface marker combination in adipose tissue of HIV-positive diabetics compared with HIV-negative diabetics and HIV-positive non-diabetics. These C-G-C$^+$ CD4$^+$ T cells can be virus specific, as demonstrated by CMV tetramer staining; fall largely within the T_{EM} and T_{EMRA} subsets; and have a pro-inflammatory and cytotoxic RNA transcriptome signature. In contrast, HIV-negative diabetics had a larger proportion of CD69$^+$ CD4$^+$ T cells in adipose tissue that were largely T_{EM} cells and expressed gene transcriptomes that regulate metabolism and inflammation. CD69$^+$ CD4$^+$ and CX3CR1$^+$ CD4$^+$ T cells in adipose tissue had more clonal TCR repertoires compared with the same cells in blood, suggesting that these cells may undergo antigen-stimulated expansion in the tissue compartment. Our findings suggest that expansion of adipose tissue memory CD4$^+$ T cells may be exaggerated in HIV-positive persons, a group characterized by heightened chronic innate and adaptive immune activation and a disproportionately higher risk of developing metabolic disease.

RESULTS

CX3CR1$^+$ GPR56$^+$ CD57$^+$ (C-G-C$^+$) CD4$^+$ T cells are enriched in adipose tissue of HIV-positive diabetics and include CMV-specific cells

We first assessed the proportion of CD69$^+$ and CD69$^-$ C-G-C$^+$ CD4$^+$ T cells in adipose tissue and blood from HIV-positive non-diabetic, pre-diabetic, and diabetic participants as performed in our prior studies using multiparametric flow cytometry (STAR methods; Figures S1A and S1B).[7] Concatenated uniform manifold approximation and projection (UMAP) and t-distributed stochastic neighbor embedding (t-SNE) identified two distinct subpopulations of CD69$^+$ CD4$^+$ and CD69$^-$ C-G-C$^+$ CD4$^+$ T cells in non-diabetic adipose tissue (14.7% and 7.1%, respectively), which increased as a proportion of total CD4$^+$ memory T cells with progressive glucose intolerance in pre-diabetics (26.6% and 6.0%, respectively) and HIV-positive diabetics (30.6% and 14.5%, respectively; Figure 1A). There were far fewer CD69$^+$ CD4$^+$ cells in paired blood samples (2.6% in non-diabetics, 4.2% in pre-diabetics, and 4.1% in diabetics). In contrast, the proportions of C-G-C$^+$ CD4$^+$ T cells in blood were similar to adipose tissue and also increased with progressive glucose intolerance (4.8% in non-diabetics, 7.7% in pre-diabetics, and 14.5% in diabetics; data not shown).

Adipose tissue CD69$^+$ CD4$^+$ T cells were predominantly T_{EM} (68.6%) and fewer T_{CM} (21.7%) and T_{EMRA} (6.1%) cells (Figures 1B and 1C). In contrast, adipose tissue CX3CR1$^+$ GPR56$^+$ CD4$^+$ cells were predominantly T_{EMRA} (54.7%) and T_{EM} (35.8%) cells (CD57 was not included in this analysis). Peripheral blood CD69$^+$ CD4$^+$ T cells had a higher proportion of T_{CM} (43.4%) to T_{EM} cells (25.0%). Peripheral CX3CR1$^+$ GPR56$^+$ CD4$^+$ T cells averaged 4.4% T_{CM}, 48.5% T_{EM}, and 43.1% T_{EMRA} cells, respectively.

CX3CR1 and GPR56 expression has been described on CMV-specific T cells.[16,20,21,27–29] We used human leukocyte antigen (HLA)-DR7 tetramers against human cytomegalovirus (HCMV) gB$_{217–227}$ | DYSNTHSTRYV (DYS) to identify T cells specific to this CMV antigen in the peripheral blood of participants with HLA-DR7 (adipose tissue T cells could not be assayed because of a limited supply of adipose tissue samples). We found that 92%–98% of DYS tetramer$^+$ CD4$^+$ cells also expressed the C-G-C surface marker combination (Figures 1D and 1E).

Adipose tissue CD4$^+$ memory T cell transcriptomes differ by HIV status

The increasing proportion of adipose tissue C-G-C$^+$ CD4$^+$ T cells with progressive glucose intolerance in HIV-positive participants led us to ask whether this finding was specific to HIV infection. To address this, we analyzed adipose tissue samples from five HIV-negative diabetics and six closely matched HIV-positive diabetics (Table S1). All 11 participants were CMV positive. We found that a larger proportion of adipose tissue CD4$^+$ T cells from HIV-positive diabetics expressed the C-G-C combination compared with HIV-negative diabetics (23% versus 3%, p < 0.05; Figures 2A and 2B, column i). In contrast, CD69$^+$ CD4$^+$ T cells were more common in adipose tissue of HIV-negative diabetics (54% versus 28% in HIV-positive persons, p = 0.18). Notably, there was no difference in the combined proportion of CD69$^+$ CD4$^+$ and C-G-C$^+$ CD4$^+$ T cells between HIV-positive and HIV-negative diabetics (Figure 2B, column iii).

We next performed scRNA-seq on index-sorted CD3$^+$ memory T cells (adipose tissue and matched peripheral blood mononuclear cell [PBMC] samples) from HIV-positive and HIV-negative diabetics, with good representation of CD4$^+$ and CD8$^+$ T cells from all study participants (Figures S2A and S2B), and
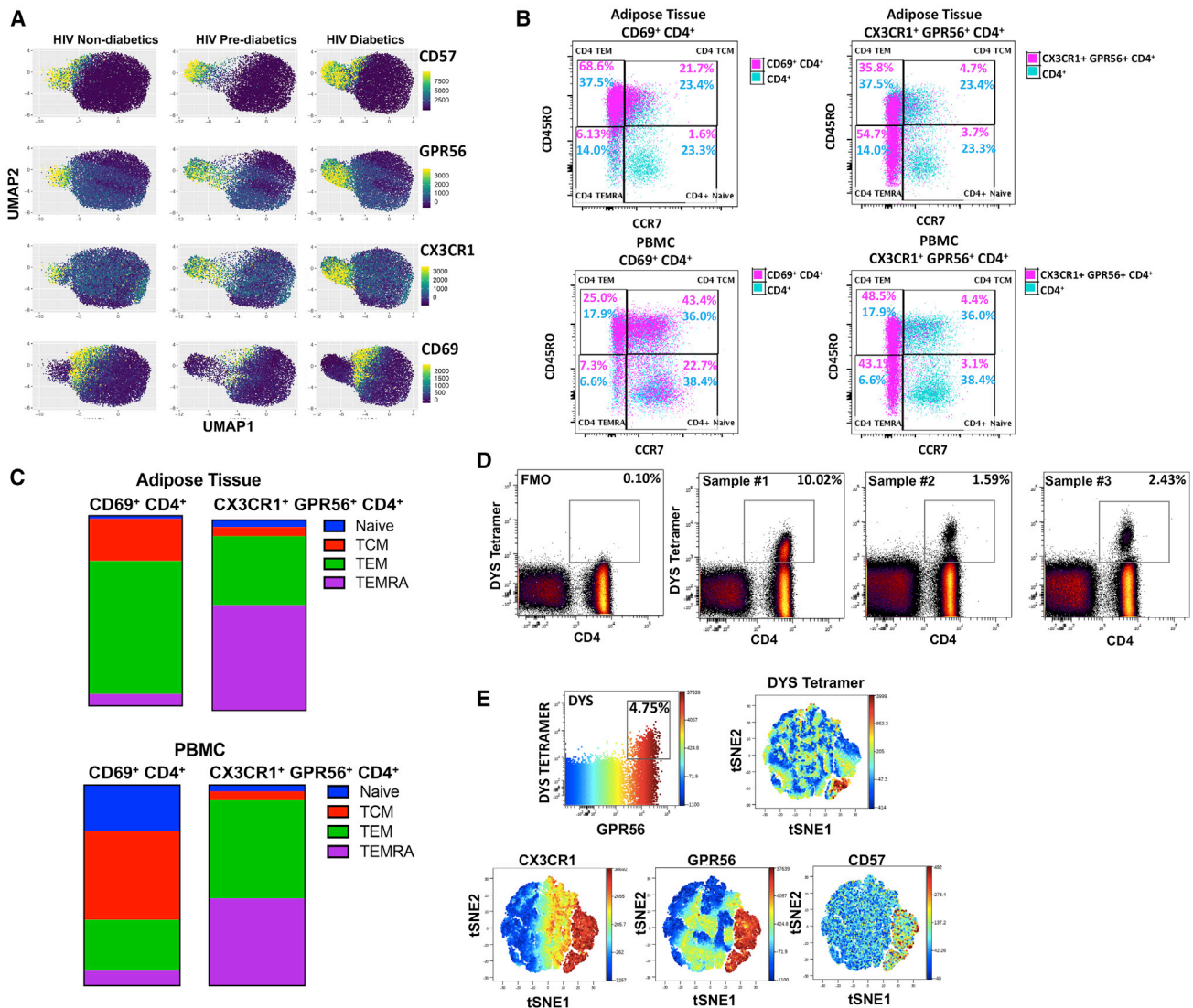
Figure 1. C-G-C$^+$ CD4$^+$ T cells are enriched in adipose tissue of HIV-positive diabetics and include CMV-specific cells

(A) Concatenated UMAP plots of adipose tissue CD4$^+$ T cells show surface marker expression (CD57, GPR56, CX3CR1, and CD69) in HIV-positive non-diabetic (n = 11), pre-diabetic (n = 7), and diabetic (n = 6) participants.

(B) Concatenated flow cytometry plots (n = 26) show the distribution of naive, central memory (T$_{CM}$), effector memory (T$_{EM}$), and effector memory CD45RA+ (T$_{EMRA}$) cells within CD69$^+$ CD4$^+$ and CX3CR1$^+$ GPR56$^+$ CD4$^+$ T cell subsets (pink) in adipose tissue and peripheral blood mononuclear cells (PBMCs); CD57 expression is not shown. These plots overlay the memory subset distribution of total CD4$^+$ T cells (turquoise).

(C) The relative proportions CD69$^+$ CD4$^+$ T$_{EM}$ and CX3CR1$^+$ GPR56$^+$ CD4$^+$ T$_{EMRA}$ cells were higher in adipose tissue compared with blood. PBMCs from HLA-DR7$^+$ HIV-positive persons were stained with a 12-antibody panel that included the human CMV tetramer (HCMV gB$_{217-227}$ | DYSNTHSTRYV [DYS]).

(D) PBMCs from HLA-DR7$^+$ HIV-positive persons were stained with a 12-antibody panel that included the human CMV tetramer (HCMV gB$_{217-227}$ | DYSNTHSTRYV [DYS]). Three representative samples of 5 total are shown.

(E) The distribution of DYS tetramer$^+$ cells are displayed in a two-dimensional plot colored according to GPR56 expression, and CD4$^+$ DYS tetramer$^+$ cells are also shown in visualization of t-distributed stochastic neighbor embedding (viSNE) plots, demonstrating co-expression of CX3CR1, GPR56, and CD57.

See also Figure S1.

calculated differential gene expression (Table S2). Adipose tissue CD4$^+$ T cells from HIV-positive diabetics (n = 2, 190 cells) and HIV-negative diabetics (n = 5, 483 cells) that were processed and sequenced simultaneously were used for these comparisons to avoid differences due to batch effect. We first performed differential expression analysis using a panel of immune genes

(Table S3; Figure 2C). The top genes highly expressed in CD4$^+$ memory T cells from HIV-positive diabetics compared with HIV-negative diabetics (p < 0.05) enriched for several pathways, including the TCR signaling pathway; the Th1, Th2, and Th17 cell differentiation pathways; and the nuclear factor κB (NF-κB) signaling pathway (Figure 2D). There were too few immune

A

B

C Adipose tissue T cell gene expression

D Enriched pathways in adipose tissue CD4⁺ T cells in HIV-positive with diabetes

E Perivascular adipose tissue CD4 and CX3CR1 staining
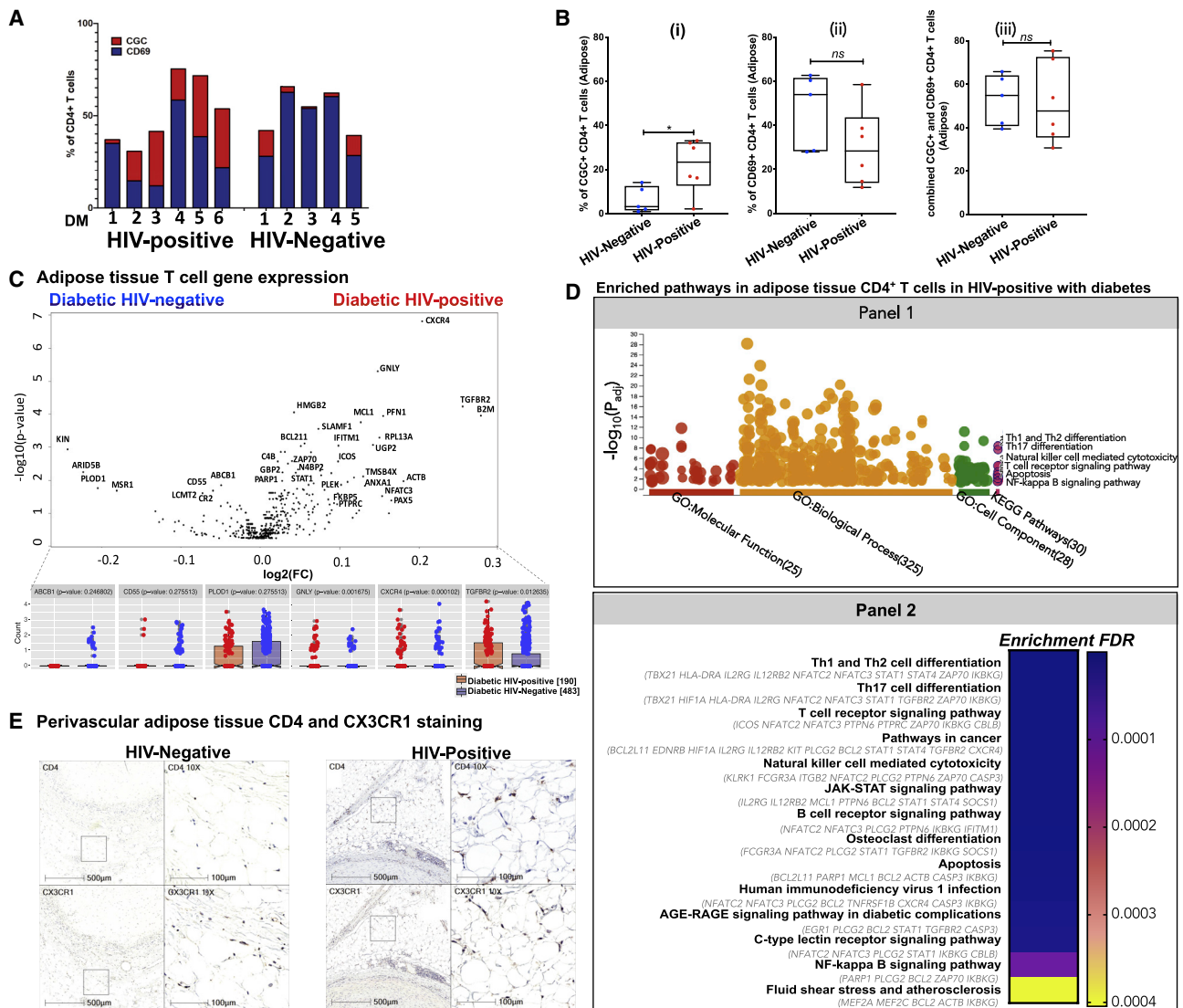

Figure 2. Adipose tissue CD4⁺ T cell transcriptomes differ by HIV status, and CD4⁺ T cells are more commonly C-G-C⁺ in HIV-positive versus CD69⁺ in HIV-negative persons

(A) Adipose tissue CD4⁺ T cells from six HIV-positive and five HIV-negative diabetics were stained with the 12-antibody panel and analyzed by flow cytometry. The bar chart shows the distribution of adipose C-G-C⁺ CD4⁺ T cells and CD69⁺ CD4⁺ T cells by HIV status.

(B) We quantified (i) C-G-C⁺ CD4⁺ T cells, (ii) CD69⁺ CD4⁺ T cells, and (iii) the combination of the two subsets.

(C) scRNA-seq was performed on adipose tissue CD4⁺ memory T cells from HIV-positive (n = 2) versus HIV-negative diabetics (n = 5) on the same sequencing run, and differential gene expression was assessed using a panel of immune genes.

(D) Gene enrichment pathway analysis was performed on differentially expressed genes higher in adipose tissue CD4⁺ T cells from HIV-positive diabetics with p < 0.05. Genes higher in HIV-negative diabetics did not enrich for Kyoto Encyclopedia of Genes and Genomes (KEGG) pathways (data not shown).

(E) Immunohistochemical stains of serial sections of perivascular adipose tissue show that CD4⁺ and CX3CR1⁺ cells are present in the adipose tissue of HIV-negative and HIV-positive diabetics. The p values were determined by Mann-Whitney U test and differential gene expression by Kruskal-Wallis test. Pathway enrichment analysis was performed using the web-based g:Profiler (version e100_eg47_p14_7733820, panel 1) and ShinyGO (v.0.61, panel 2). Analysis in g:Profiler was performed using the g:SCS method for multiple testing correction with an experiment-wide threshold of a = 0.05; *p < 0.05.

See also Figures S1 and S2 and Table S2.

genes with higher expression in adipose tissue CD4⁺ T cells from HIV-negative diabetics to perform a similar pathway analysis.

Differential gene expression of all transcripts, including non-immune genes, was also performed (Figure S3A). The genes higher in adipose tissue CD4⁺ T cells from HIV-positive diabetics

enriched for the Th17 differentiation pathway (Figure S3B). In contrast, genes overexpressed in CD4⁺ T cells from HIV-negative diabetics did not enrich for any Kyoto Encyclopedia of Genes and Genomes (KEGG) or Gene Ontology (GO) biological process pathways. A similar analysis of PBMC CD4⁺ T cells from HIV-

positive diabetics versus HIV-negative diabetics also enriched for the interleukin-17 (IL-17) signaling pathway (Figure S3C).

Last, we obtained serial autopsy sections of coronary arteries with adjacent perivascular fat from HIV-positive and HIV-negative donors to confirm the presence of immune cells in adipose tissue by histology, and ensure that these cells did not represent contamination from blood. CD4$^+$ and CX3CR1$^+$ cells were present in perivascular adipose tissue in close contact with adipocytes (Figure 2E). Because of immunohistochemical staining of serial sections, there is no direct overlap between CD4 and CX3CR1 staining in the images. However, the assay shows that cells expressing both of these surface markers are present in adipose tissue.

In summary, we found that C-G-C$^+$ CD4$^+$ T cells were more common in fat of HIV-positive diabetics. The CD4$^+$ memory T cell gene transcriptomes enriched for pathways involved in IL-17 differentiation and signaling. On the other hand, CD69$^+$ CD4$^+$ T cells predominated in HIV-negative diabetics and no enriched pathways were observed.

Adipose tissue CD4$^+$ T cells from HIV-positive non-diabetics and diabetics cluster based on RNA transcriptomes

We used the UMAP dimension reduction technique to visualize adipose tissue CD4$^+$ T cells from HIV-positive non-diabetics and diabetics based on transcriptomic gene expression. These appeared to separate by diabetes status, with areas of overlap (Figure 3A). We performed unsupervised K-means clustering to group cells using an iterative approach. Seven was the maximum number of assigned clusters. Using one-way ANOVA, a number of immune genes were differentially expressed by the cells in all seven clusters (Figure 3B; Table S4). Cluster 5 had higher expression of CD69, whereas CX3CR1 gene expression appeared to be higher in cluster 6 but was not statistically significant. Differential gene expression between cluster 5 and 6 confirmed higher expression of CD69 in the former, along with IL7R, CCR7, CD27, CD55, and CD44. Genes higher in cluster 6 included CCL5, GNLY, NKG7, FGFBP2, GZMB, GZMH, IFITM1, and CCL4 (Figure 3C; Table S4). The differential gene expression between cluster 3 (predominantly HIV-positive diabetics) and cluster 5 was notable for higher LCMT2, SOX11, CD47, HSPA4, NCAM1, KCNJ2, and GZMA in cluster 5 compared with higher TNFAIP3, CD69, CD55, TGFB1, FOS, and JUN in cluster 3 (Figures 3D and 3E; Table S4).

Adipose tissue CD4$^+$ T cells from HIV-positive diabetics have a cytotoxic RNA transcriptome signature compared with those from HIV-negative diabetics

Our unsupervised UMAP analysis of adipose tissue CD4$^+$ T cells demonstrated clusters of transcriptionally distinct cells in HIV-positive non-diabetics versus diabetics, so we next assessed T cell differential gene expression and response to antigen in these two groups. Overall, HIV-positive diabetics had a higher combined proportion of adipose tissue CD69$^+$ and C-G-C$^+$ CD4$^+$ T cells compared with non-diabetics (47.6% versus 21.2% of total CD4$^+$ memory T cells, p = 0.03) (Figure 4A) as reported previously.[7] We then assessed differential expression of immune genes expressed by adipose tissue CD4$^+$ memory

T cells, irrespective of CD69 or C-G-C expression, from HIV-positive non-diabetics versus diabetics (Figure 4B; Table S5). Genes higher in HIV-positive diabetics included AGER, CD47, PRF1, GZMA, GZMB, and GZMH. In contrast, adipose tissue CD4$^+$ T cells from non-diabetics had higher levels of CD55, IL10R, TGFB1, KLF3, and S1PR1. Immune genes expressed in both adipose tissue and blood CD4$^+$ T cells of non-diabetics included MX1, TGFB1, BIRC2, IL6R, IL23R, and PLOD1. However, adipose tissue and blood CD4$^+$ T cells from diabetics overexpressed a greater number of overlapping immune genes, including TGFBR2, GNLY, GZMH, GZMB, GZMA, NCAM1, and SOX11 (Figure 4C; Table S5), which enriched for cytolysis and granzyme-mediated apoptotic pathways (Figure 4D).

We also assessed the functional response to antigen using PBMCs from HIV-positive non-diabetics (n = 15) versus diabetics (n = 8); adipose tissue T cells could not be assayed because of insufficient samples (Figure 4E; Figure S4). Similar to the gene transcripts, CD4$^+$ T cells from diabetics had higher expression of granzyme B at baseline and expressed higher levels of interferon-γ and tumor necrosis factor alpha (TNF-α) after stimulation with a staphylococcal enterotoxin B (SEB) and CMV phosphoprotein 65 (pp65) peptide pool (Figures 4F and 4G). Granzyme B is a serine protease that is expressed in cytotoxic lymphocytes contained in granules along with perforin. Stimulation of T cells via TCR leads to formation of an immunological synapse and release of the contents of the granules. Similar to a previous study,[30] not all granzyme B$^+$ T cells expressed inflammatory cytokines upon stimulation. Finally, we obtained autopsy samples of coronary arteries with adjacent perivascular fat from two HIV-positive donors, with and without a recorded diagnosis of diabetes prior to death, for granzyme B immunohistochemistry staining. Granzyme B$^+$ cells were present in the perivascular adipose tissue of HIV-positive diabetics, and these appeared to be more numerous than in HIV-positive non-diabetics (Figure 4H). Statistical analysis was not performed because of the small number of samples available for each group (Table S1).

Adipose tissue CX3CR1$^+$ CD4$^+$ T cells have pro-inflammatory gene transcriptomes

To understand the contribution of CX3CR1$^+$ CD4$^+$ T cells to the cytotoxic RNA transcriptome observed for total adipose tissue CD4$^+$ memory T cells in HIV-positive diabetics, we compared adipose tissue CX3CR1$^+$ and CX3CR1$^-$ CD4$^+$ T cells stratified by diabetes status. Applying p < 0.1 as a threshold, there were 124 genes higher in CX3CR1$^+$ CD4$^+$ T cells from HIV-positive nondiabetics, including HLA-A, HLA-B, IFNGR1, PSMB9, and CD52. These enriched for the Th17 differentiation, nucleotide-binding oligomerization domain (NOD)-like receptor signaling, and TCR pathways (Figure 5A; Table S5). A similar analysis of HIV-positive diabetics identified 61 genes with higher expression in CX3CR1$^+$ CD4$^+$ T cells, including IKBKB, PDGFA, AGER, and CD160, which also enriched for the Th17 differentiation, mitogen-activated protein kinase (MAPK), and FoxO signaling pathways (Figure 5B; Table S5). Notably, HIV-negative diabetics had fewer CX3CR1$^+$ CD4$^+$ T cells, but in comparison with CX3CR1$^-$ CD4$^+$ T cells, these enriched for the NOD-like receptor signaling, focal adhesion program, and advanced glycation end
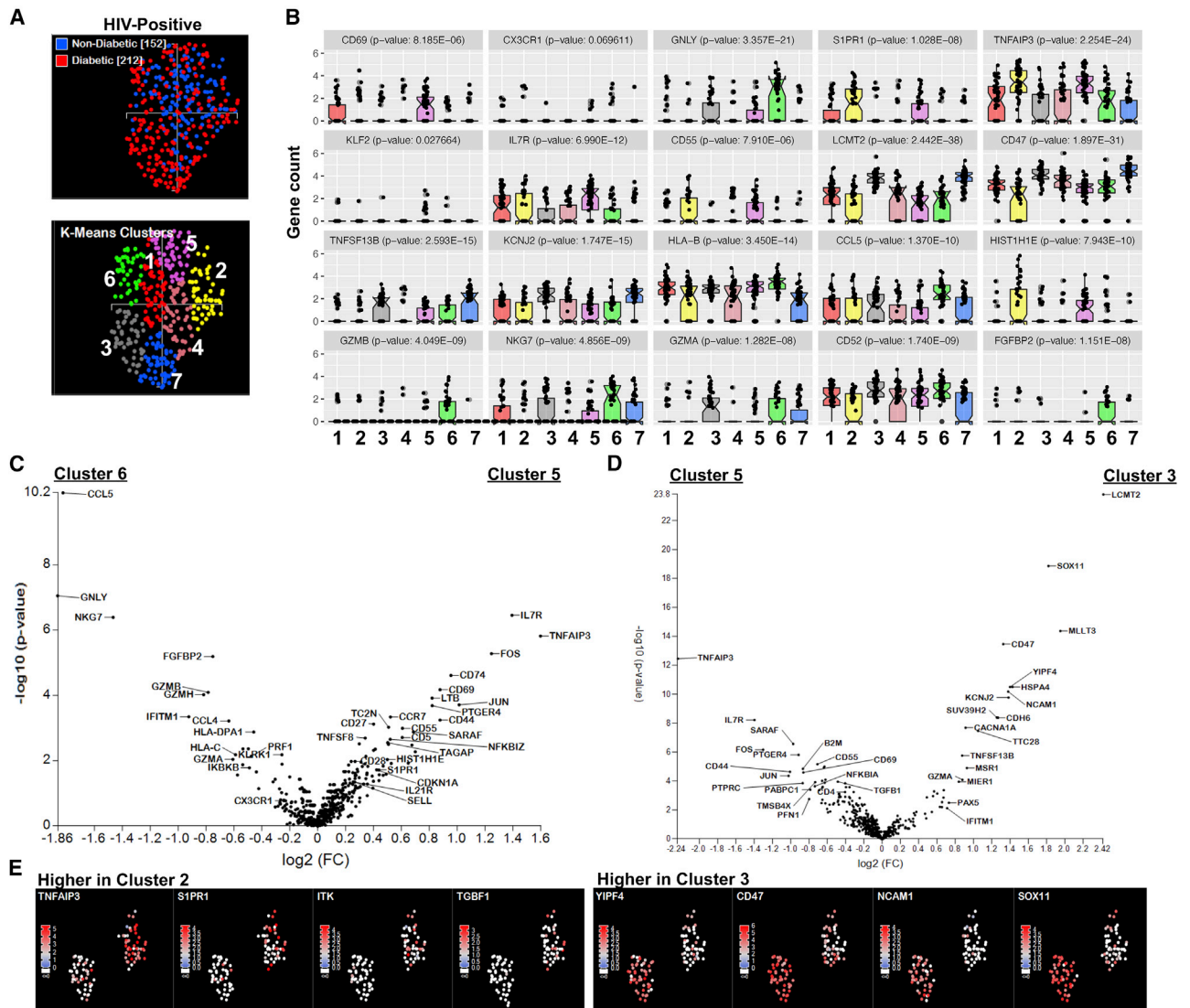
Figure 3. Unsupervised analysis of adipose tissue CD4⁺ T cells from HIV-positive non-diabetics and diabetics reveals clusters of transcriptionally distinct cells

(A) UMAPs showing adipose tissue CD4⁺ T cells from HIV-positive non-diabetics and diabetics and cell clusters using the K-means algorithm.

(B) Boxplots show gene counts that were significantly higher in different cell clusters, with adjusted p values indicated next to the gene.

(C and D) Volcano plot showing differential gene expression between cluster 5 (higher CD69 gene expression) and cluster 6 (higher CX3CR1 gene expression) (C) and between cluster 3 (predominantly cells from HIV-positive diabetics) and cluster 5 (predominantly cells from HIV-positive non-diabetics) (D).

(E) Heatmaps of select genes differentially expressed in cluster 2 (predominantly non-diabetic HIV-positive) and cluster 3 (predominantly diabetic HIV-positive) are shown in UMAPs.

Differential gene expression was performed by Kruskal-Wallis test. See also Figure S3 and Table S4.

products and their receptors (AGE-RAGE) signaling pathways (a contributor to diabetic complications).

CX3CR1⁺ CD4⁺ T cells from all three groups had higher LIM and cysteine-rich domain protein 1 (*LMCD1*) gene transcripts than CX3CR1⁻ CD4⁺ T cells (Figure S5; Table S5). *LMCD1* is a transcriptional factor that represses *GATA-6* mediated *trans*-activation of cardiac and lung tissue-specific promoters and is important for development of cardiac hypertrophy.[31] Other notable overlapping genes that were highly expressed in CX3CR1⁺ CD4⁺ T cells from diabetics (HIV-positive and HIV-

negative) were *PDGFA*, *TGFB3*, and *RAB27A*. The GO biological processes enriched by these genes are blood coagulation/hemostasis and wound healing (false discovery rate [FDR] < 0.05 for both).[32] These data suggest that CX3CR1⁺ CD4⁺ T cells are pro-inflammatory irrespective of diabetes or HIV status.

We performed similar analyses to assess adipose tissue CD69⁺ CD4⁺ T cell transcriptomes (Figures S6; Table S5). CD69 is a marker of early activation, tissue residency, and T helper cell differentiation.[33] The core gene signature of CD69⁺ tissue resident memory cells has been well established and
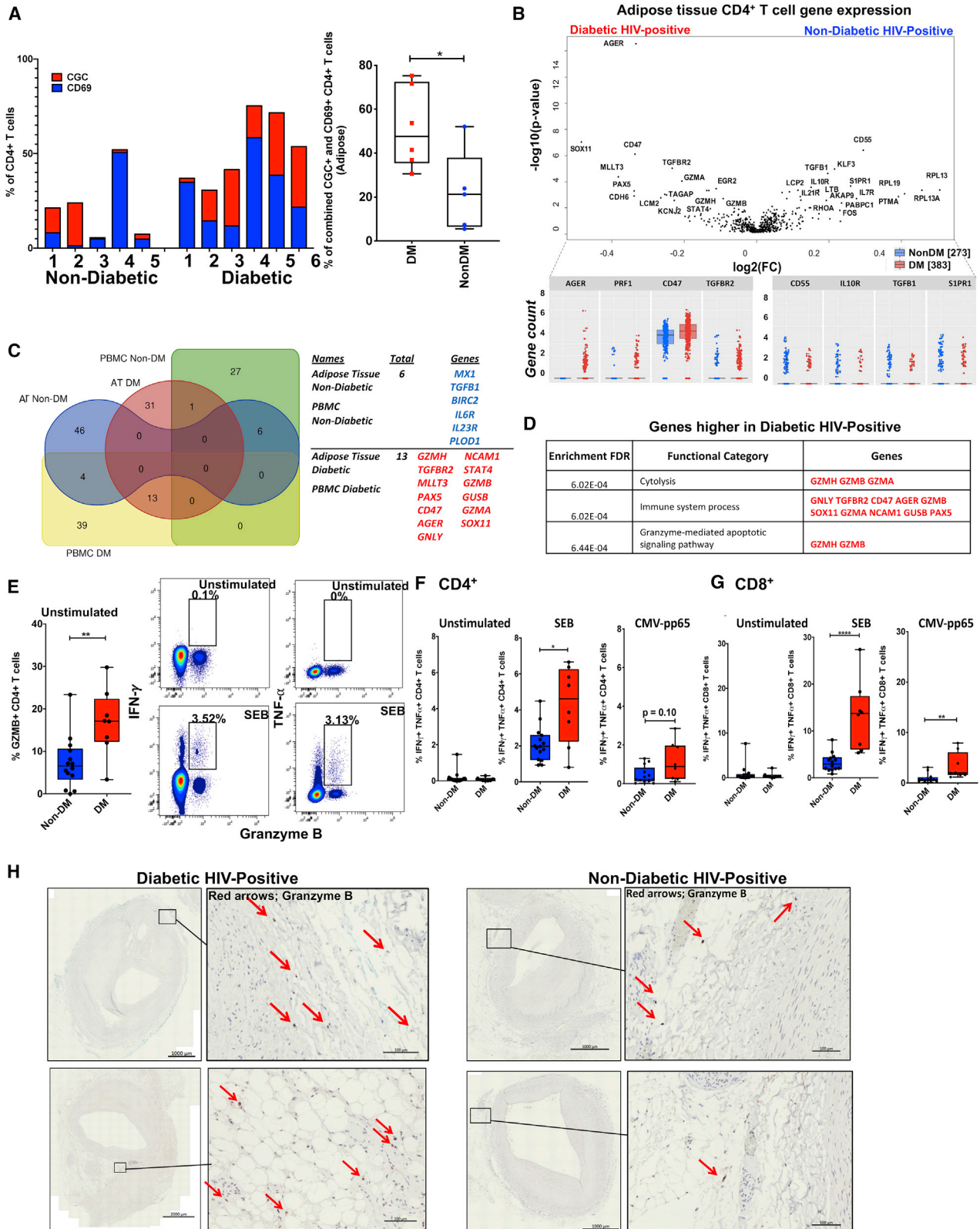
(legend on next page)

includes *IL-2*, *IL-10*, *PD-1*, *RGS1*, *CXCR6*, and *ITGAE*.[34] None of these previous analyses were of HIV-positive persons or adipose tissue T cells. Using p < 0.1 as a threshold, genes higher in CD69^{+} CD4^{+} T cells from HIV-positive non-diabetics enriched for the apelin signaling (*GNAQ*, *NOS2*, and *ITPR1*) and arginine biosynthesis (*NOS2* and *ARG2*) pathways (Figure S6A); HIV-positive diabetics enriched for the NF-κB signaling (*MALT1*, *MYD88*, *TRAF3*, and *TNFSF14)* and MAPK signaling (*KIT*, *MYD88*, and *PDGFA)* pathways (Figure S6B). Last, CD69^{+} CD4^{+} T cells from HIV-negative diabetics expressed *CD47*, *CD52*, *CDC42*, *OAZ1*, *CD69*, *CD6*, and *NCF4*. These did not enrich for any KEGG pathways (Figure S6C). There were three overlapping genes highly expressed by adipose tissue CD69^{+} CD4^{+} T cells from HIV-positive non-diabetics and diabetics (*CDH6* [cadherin 6 calcium-dependent cell adhesion protein]; *SLC25A37*, also known as Mitoferrin-1 and a mitochondrial iron transporter; and *KLRD1-CD94*, a receptor for recognition of major histocompatibility complex [MHC] class I HLA-E molecules). In summary, these findings suggest that CX3CR1^{+} CD4^{+} T cells in HIV-positive persons have gene transcripts involved in Th17 differentiation irrespective of diabetes status. However, this was not the case for CX3CR1^{+} cells from HIV-negative persons. CD69^{+} CD4^{+} T cells, on the other hand, had fewer genes that were overexpressed compared with CD69^{−} CD4^{+} T cells in all three groups.

C-G-C^{+} CD4^{+} T cells and CD69^{+} CD4^{+} T cells have distinct RNA transcriptomes that differ in HIV-positive diabetics and non-diabetics

Using dimensional reduction analysis of adipose tissue CD4^{+} T cell surface marker expression, CD69^{+} and C-G-C^{+} CD4^{+} T cells are non-overlapping subsets (Figure 1A). We performed differential gene expression of adipose tissue CD69^{+} and C-G-C^{+} CD4^{+} T cells in HIV-positive diabetics (Figure 6A; Table S5); genes shown in blue (n = 25) were higher in adipose tissue CD69^{+} CD4^{+} T cells, whereas genes shown in red (n = 55) were higher in C-G-C^{+} CD4^{+} T cells. The top three KEGG pathways enriched in CD69^{+} cells were the NOD-like receptor signaling, NF-κB signaling, and retinoid acid-inducible gene-I (RIG-I)-like receptor signaling pathways (Figure 6B). C-G-C^{+} CD4^{+} T cell genes enriched for the C-type lectin, FoxO signaling, and MAPK signaling pathways (Figure 6C). The GO biological processes enriched by the genes from CD69^{+} CD4^{+} T cells (*MALT1*, *TMEM173*, *PYCARD*, *KLRD1*, *LAG3*, *TRAF3*, *MYD88*,

RIPK1, *NCAM1*, and *HLA-C*) were in the innate immune response process. Genes from C-G-C^{+} CD4^{+} T cells enriched for leukocyte activation and immune system processes (*CD4*, *CD5*, *LEF1*, *ITGA4*, *CD40LG*, *CD160*, *IL15*, *RHOA*, *BCL3*, *CTSC*, *LDLR*, *ITGB2*, *CASP3*, *CD6*, *NFATC2*, *IL21R*, *C3*, *CD53*, *PLAC8*, *CTSS*, *PPIA,* and *IGF2R*) (Figure 6D). Notably, Toll-like receptors and NOD-like receptors have been implicated in the pathogenesis of diabetes through activation by gut microbiota and free fatty acids.[35]

We performed a similar analysis in HIV-positive non-diabetics and identified 76 genes that were higher in C-G-C^{+} CD4^{+} T cells versus 9 genes in CD69^{+} CD4^{+} T cells (Table S5). Genes higher in C-G-C^{+} CD4^{+} T cells enriched for several KEGG pathways, including NOD-like receptor signaling and Toll-like receptor signaling (Figure S7A). Genes higher in CD69^{+} CD4^{+} T cells did not enrich for any KEGG pathways. The GO biological processes enriched in C-G-C^{+} CD4^{+} T cells were similar to those of HIV-positive diabetics, including leukocyte activation (Figure S7B). Notably, gene transcripts that were highly expressed in C-G-C^{+} CD4^{+} T cells from HIV-negative diabetics enriched for the RIG-I-receptor signaling and complement cascade pathways (Figure S7C). Similar to HIV-positive non-diabetic and diabetics, the GO biological processes were related to immune activation and defense processes (Figure S7D; Table S5).

Adipose tissue CD69^{+} and CX3CR1^{+} CD4^{+} memory T cells are more clonal compared with CD69^{−} CX3CR1^{−} CD4^{+} memory T cells and paired cells from blood

Previous studies have reported increased TCR clonality in CD4^{+} T$_{EMRA}$ subsets compared with T$_{EM}$ and T$_{CM}$.[36] Greater clonality is a feature of TCR-dependent expansion, and the higher proportion of CX3CR1^{+} T$_{EMRA}$ suggests that these cells should be more clonal compared with CD69^{+} and other (e.g., CD69^{−} CX3CR1^{−}) CD4^{+} memory T cells. Therefore, we next assessed TCR clonality in HIV-positive participants by sorting CD4^{+} memory T cells in bulk from paired adipose tissue and blood (Figure S1A) into three groups based on expression of CD69, CX3CR1, or a lack of either marker (CD69^{−} CX3CR1^{−}) and performed DNA-based TCR sequencing (Adaptive Biotechnologies). We included CD8^{+} memory T cells for comparison.

CD69^{+} and CX3CR1^{+} CD4^{+} memory T cells in adipose tissue were more clonal compared with those expressing the

---

Figure 4. Adipose tissue CD4^{+} T cells in HIV-positive diabetics have a cytotoxic RNA transcriptome signature

(A) Bar plot and boxplot showing a higher combined proportion of CD69^{+} and C-G-C^{+} CD4^{+} T cells in adipose tissue of HIV-positive diabetics (n = 6) versus non-diabetics (n = 5).

(B) Differential gene expression of immune genes by adipose tissue CD4^{+} T cells from diabetics (n = 6, 354 cells) were compared with non-diabetics (n = 4, 273 cells).

(C) Venn diagram showing overlap of genes with higher expression (p < 0.05) in matched adipose tissue and blood CD4^{+} T cells from diabetics versus non-diabetics.

(D) GO processes enriched by overlapping genes differentially expressed by adipose and blood CD4^{+} T cells from diabetics.

(E) Intracellular cytokine staining (ICS) showing the percentage of granzyme B^{+} blood CD4^{+} T cells in HIV-positive non-diabetics (n = 15) and diabetics (n = 8) in unstimulated samples as well as co-expression of interferon γ (IFN-γ) and tumor necrosis factor alpha (TNF-α) with granzyme B after stimulation with staphylococcal enterotoxin B (SEB).

(F and G) Percentage of IFN-γ and TNF-α co-expression by CD4^{+} T cells (F) and CD8^{+} T cells (G) after SEB and CMV-pp65 peptide pool stimulation.

(H) Immunohistochemistry stains showing granzyme B^{+} cells in perivascular adipose tissue of HIV-positive diabetics (n = 2) versus non-diabetics (n = 2).

Differential gene expression was determined by Kruskal-Wallis test. Mann-Whitney *U* test was used to compare cytokine expression. *p < 0.05, **p < 0.01, ****p < 0.0001. See also Figure S4 and Table S5.
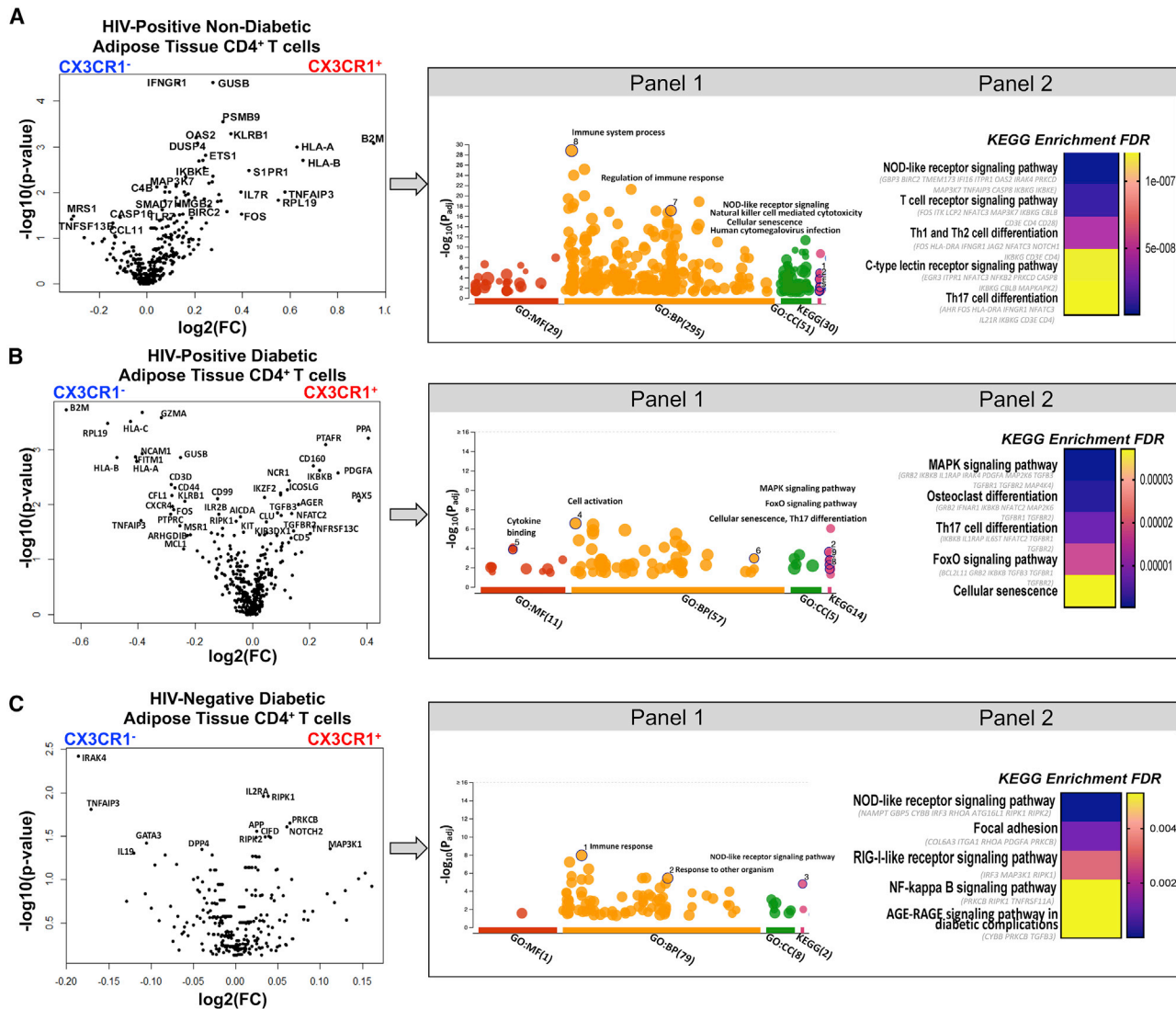
Figure 5. Adipose tissue CX3CR1⁺ CD4⁺ T cells have a pro-inflammatory transcriptome profile regardless of diabetes or HIV status

(A–C) Differential gene expression of immune genes between index-sorted CX3CR1⁺ CD4⁺ and CX3CR1⁻ CD4⁺ T cells. Top genes (p < 0.1) expressed in CX3CR1⁺ CD4⁺ T cells were used for gene enrichment analysis. Two panels (1 and 2) show KEGG pathways enriched by top genes expressed by adipose tissue CX3CR1⁺ CD4⁺ T cells from HIV-positive non-diabetics (n = 5, A), HIV-positive diabetics (n = 6, B), and HIV-negative diabetics (n = 5, C). Differential gene expression was determined by Kruskal-Wallis test. Panel 1 enrichment analysis was performed using g:Profiler. Panel 2 enrichment analysis was performed using ShinyGO based on hypergeometric distribution followed by FDR correction. See also Figure S5 and Table S5.

same markers in blood (p < 0.05; Figure 7A), whereas there was no difference in clonality between adipose tissue and blood for CD69⁻ CX3CR1⁻ CD4⁺ (all other) memory T cells and CD8⁺ memory T cells. In adipose tissue, CD69⁺ and CX3CR1⁺ CD4⁺ memory T cells were significantly more clonal compared with CD69⁻ CX3CR1⁻ CD4⁺ T cells. CX3CR1⁺ CD4⁺ T cells in blood were also more clonal than CD69⁻ CX3CR1⁻ CD4⁺ T cells but CD69⁺ CD4⁺ T cells were not (Figure 7A). As expected, CD8⁺ memory T cells generally had a higher degree of clonality than CD4⁺ memory T cells.[37,38] Figure 7B shows clonality scores for matched pairs of adipose tissue and blood CX3CR1⁺, CD69⁺, and CD69⁻ CX3CR1⁻ CD4⁺ memory T cells.

We next assessed clonality scores by metabolic group (non-diabetic, pre-diabetic, and diabetic). Clonality trended higher in adipose tissue CX3CR1⁺ CD4⁺ T cells from diabetics compared with non-diabetics and pre-diabetics (p = 0.06 and p = 0.07; Figure 7C). In contrast, there was little difference between adipose tissue and blood CD69⁺ CD4⁺ memory T cell clonality between metabolic groups (Figure 7D). The CDR3 amino acid sequences from TCRs with a productive frequency greater than 5% and two or more templates are shown in Table S6.[39–51]

The CX3CR1 receptor is important for leukocyte transit across the endothelium, suggesting that CX3CR1⁺ CD4⁺ T cells may represent a population trafficking through the tissue as opposed to fixed or "resident." We compared TCRs using the Morisita
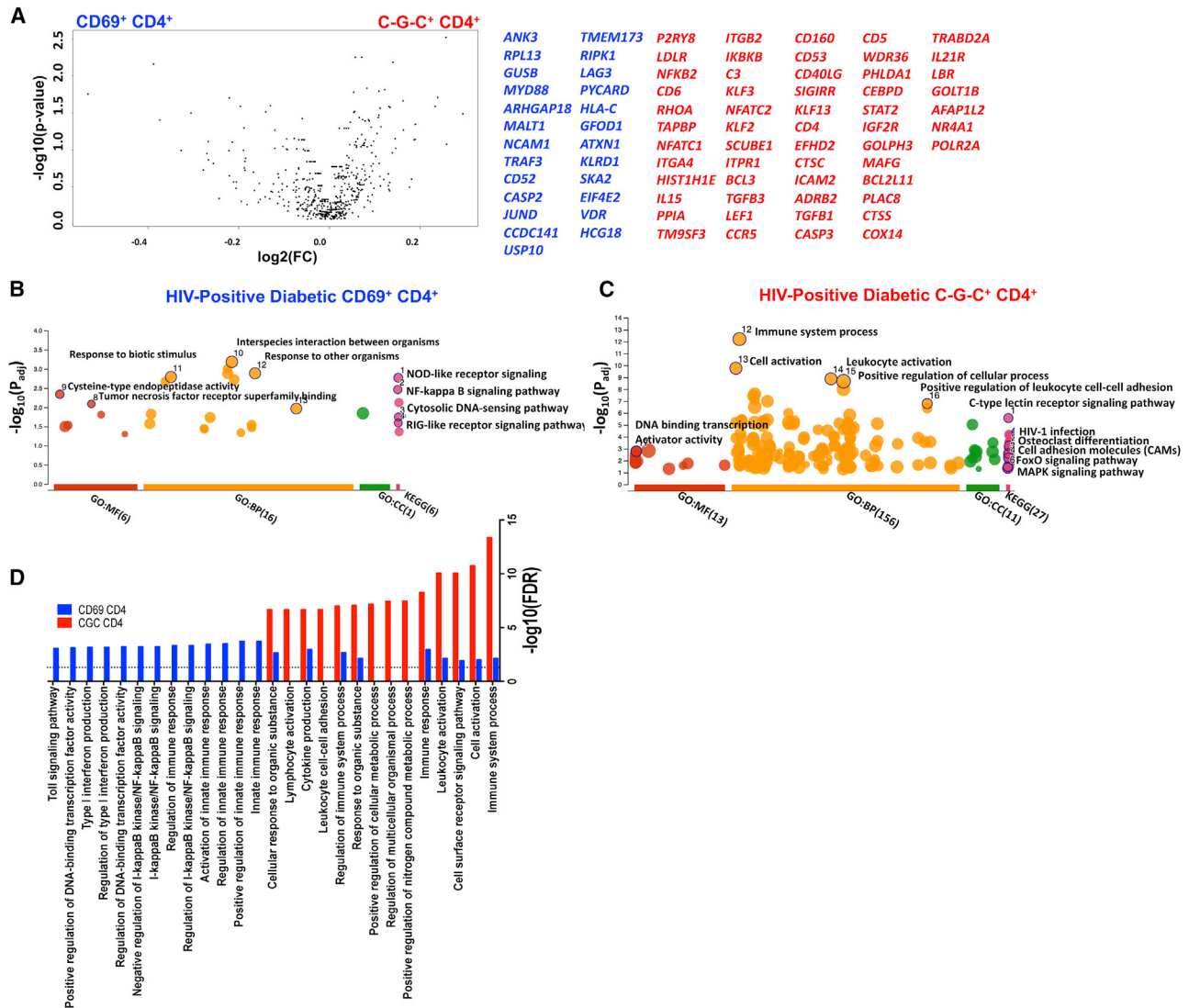
Figure 6. Characterization of C-G-C⁺ CD4⁺ T and CD69⁺ CD4⁺ T gene transcripts in HIV-positive diabetics

(A) Volcano plot showing differential gene expression of immune genes between CD69⁺ (blue) and C-G-C⁺ (red) CD4⁺ T cells from adipose tissue of HIV-positive diabetics (n = 6). Top genes (p < 0.1) were used for gene enrichment analysis.

(B and C) A Manhattan-like plot summarizes the KEGG pathways enriched by top genes expressed by adipose tissue CD69⁺ CD4⁺ T cells (B) and C-G-C⁺ CD4⁺ T cells (C).

(D) Top Gene Ontology (GO) terms enriched for genes that are differentially expressed by CD69⁺ CD4⁺ and C-G-C⁺ CD4⁺ T cells.

Differential gene expression was determined by Kruskal-Wallis test. KEGG pathway enrichment analysis was performed using g:Profiler, and GO terms were from ShinyGO. See also Figure S6–S8 and Table S5.

overlap index range (0 [unique repertoires] to 1 [complete similarity between two groups]) and found a higher degree of overlap between the TCR repertoire of adipose tissue and blood CX3CR1⁺ CD4⁺ T cells compared with CD69⁺ CD4⁺ T cells (Figure 7E). We interpret this finding to suggest that many adipose CD4⁺ CD69⁺ T cells may be "clonally segregated" from blood, reflecting a tissue-resident status, which is supported by a recent report showing clonal segregation of CD69⁺ T cell subsets between blood and tissue (lung, spleen, tonsils, and salivary glands).[34] Notably, there was a high degree of overlap in CD8⁺ memory T cells between adipose tissue and blood, suggesting that these

cells may also traffic between compartments (Figure 7E). The Morisita indices did not differ by diabetic status (data not shown).

We next performed single-cell TCR sequencing (TCR-seq) on index-sorted CD3⁺ memory T cells from 4 HIV-positive diabetics and 4 HIV-positive non-diabetics, followed by RNA transcriptome analysis as outlined (Figure S1A). Circos plots show TCR α/β pairs in adipose tissue and blood. In general, adipose tissue samples had more clonal TCRs (Figure 7F; Table S7). Of the individuals with TCR-seq data, 50% of HIV-positive non-diabetics had detectable HIV in adipose tissue by quantitative PCR, whereas 75% of HIV-positive diabetics had detectable
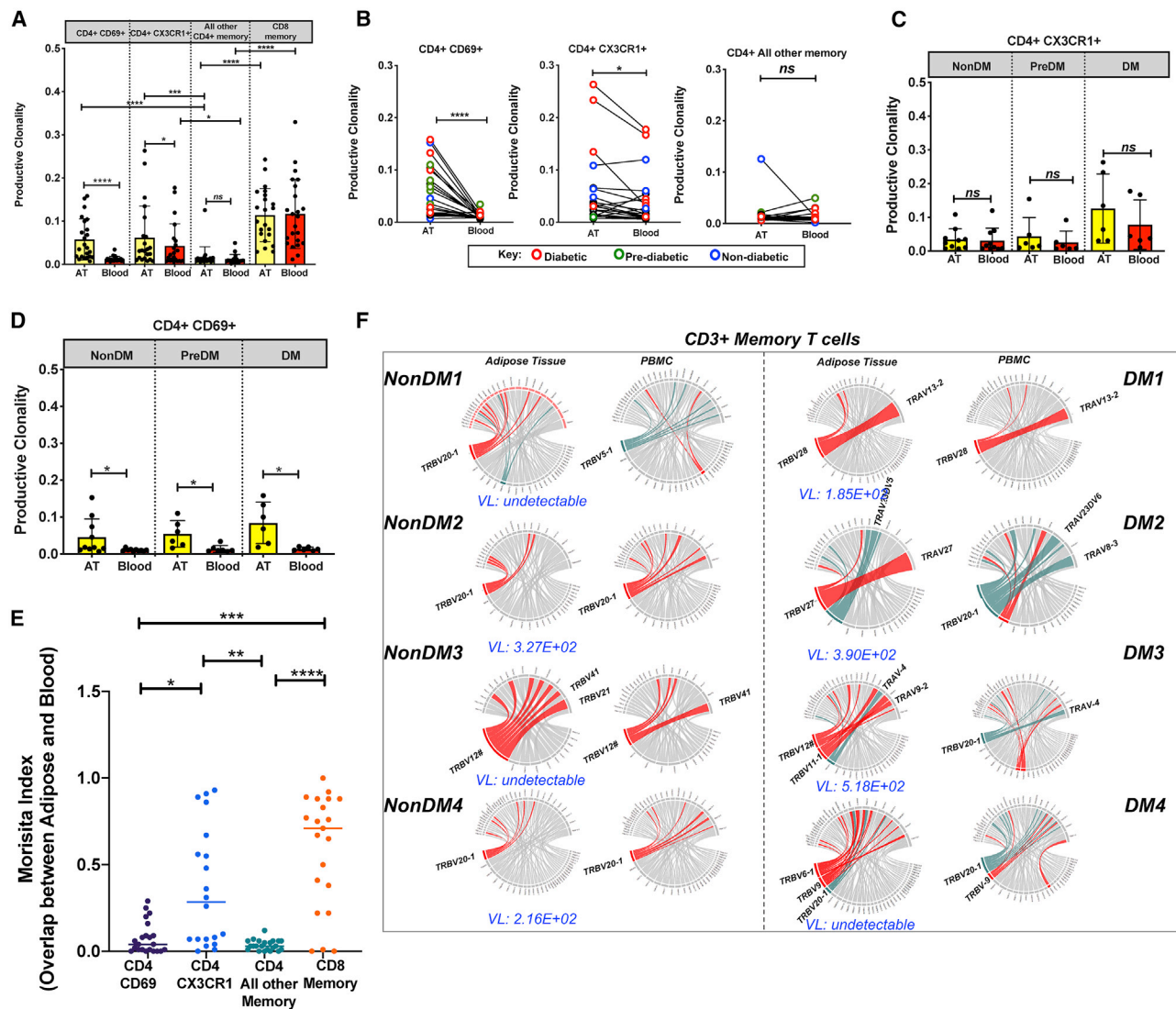
Figure 7. Adipose CD69+ and CX3CR1+ CD4+ T cells are more clonal compared with CD69− CX3CR1− CD4+ memory cells and paired cells from blood

(A) Productive T cell receptor (TCR) β clonality of bulk-sorted CD69+ CD4+ T cells, CX3CR1+ CD4+ T cells, all other (i.e., CD69− CX3CR1−) CD4+ memory T cells, and CD8+ memory T cells (n = 23 participants) from paired adipose tissue (AT; yellow) and blood (red) samples.

(B) Comparison of productive clonality in matched pairs of adipose tissue and blood CD4+ T cells, color-coded based on metabolic status (non-diabetic, blue; pre-diabetic, green; diabetic, red).

(C and D) Productive clonality compared by diabetes status (non-diabetic [non-DM], pre-diabetic [pre-DM], and diabetic [DM]) for CX3CR1+ CD4+ T cells (C) and CD69+ CD4+ T cells (D).

(E) Morisita index for overlap of TCR repertoires between matched adipose and blood samples stratified by T cell subset.

(F) Circos plots of paired TCRβ and TCRα genes of CD3+ memory T cells in adipose tissue and peripheral blood from HIV-positive non-diabetics (non-DM, n = 4) and diabetics (DM, n = 4). Red bands represent dominant TCR pairs in adipose tissue (which may also be present in blood), and turquoise bands represent dominant pairs in blood (which may also be present in adipose tissue). The HIV viral load (copies per million cells) in adipose tissue is shown in blue.

Statistical comparisons for paired samples (adipose tissue versus blood) were calculated using the Wilcoxon signed-rank test. Differences between groups were calculated using Mann-Whitney test. *p < 0.05, **p < 0.01, ***p < 0.001, ****p < 0.0001. See also Table S6.

virus. There were a few shared/public TCRs with identical CDR3 amino acid sequences on CD4+ T cells from different individuals, some of which have known epitopes. This included the known mucosal-associated invariant T cell (MAIT)-like rearrangements CAVMDSNYQLIW and CAVRDSNYQLIW (Table S7).

Last, we compared the top genes expressed by adipose tissue clonal versus nonclonal (i.e., occurring only once) TCRs on CD4+ T cells. We found that CD4+ T cells with clonal TCRs, defined as having more than two cells with the same CDR3 or TCRs shared between individuals, had higher expression of several genes associated with cytotoxic T cells. These included *CCL5*, *GNLY*, *PRF1*,

KLRG1, *GZMA*, *CX3CR1*, *TNFRSF1B*, *GZMB*, and *HLA-C* (data not shown). CD4+ T cells with non-clonal TCRs had higher expression of *SELL*, *TNFRSF9*, *GPR183*, *IL7R*, *CCR7*, *PRDM1*, *TRAF3*, *ROCK2*, *IRF8*, *IFIT3*, *RAPGEF2*, *CD55*, and *KIR3DL1*. A recent study using SELECT-seq performed a similar analysis, which identified genes expressed by clonally expanded CD8+ T cells downstream of TCR signaling, including *PRF1*, *GNLY*, *CCL5*, *KLRG1*, and *TIGIT*.[52] The similarity in genes expressed by clonal adipose tissue CD4+ T cells and those reported previously in CD8+ T cells suggests a cytotoxic phenotype that needs to be explored further.

DISCUSSION

Despite advances in effective antiretroviral therapy and durable suppression of plasma viremia, HIV-positive persons remain at higher risk of metabolic disease compared with HIV-negative individuals with similar risk factors.[8–10] Persistent inflammation is a hallmark of treated HIV infection, and elevated circulating biomarkers of inflammation are associated with an increased risk of incident diabetes in HIV-positive and -negative persons. However, the mechanisms by which immune cells contribute to development of metabolic disease are not well defined. This study evaluates adipose tissue CD4+ memory T cell phenotypes, RNA transcriptomes, and receptor clonality in the context of HIV infection and diabetes. We show that adipose tissue CD4+ T cell profiles shift with progressive glucose intolerance in HIV-positive persons, which is principally characterized by an increased proportion of C-G-C+ CD4+ T cells in HIV-positive diabetics. Furthermore, the enrichment of C-G-C+ CD4+ T cells in adipose tissue appears to be a feature of HIV infection; in comparison, CD69+ CD4+ T cells predominate in adipose tissue of HIV-negative diabetics. Although CD4+ T cells expressing C-G-C+ were primarily T_{EMRA} cells and CD69+ cells were primarily T_{EM} cells, both subsets were more clonal than CD4+ T cells lacking both markers. Furthermore, in each subset, we identified several public TCR clones in more than one participant, in addition to previously reported TCR sequences. We identified anti-CMV CD4+ T cells in the C-G-C+ population (by design, all participants in our study were CMV seropositive). Although CD4+ T cells had overlapping genes and functions, adipose tissue C-G-C+ CD4+ T cells expressed gene transcriptomes enriched for leukocyte activation and defense processes, whereas CD69+ CD4+ T cells had more genes involved in regulation of immune and metabolic processes.

Adipose tissue is a reservoir for HIV,[2,3,6,53] CMV,[23] and other viruses and bacteria.[54–57] Murine studies have demonstrated that virus replication in adipose tissue is associated with recruitment and expansion of lymphocytes independent of lymphoid organs. For example, intraperitoneal infection with lymphocytic choriomeningitis virus (LCMV) led to seeding of the adipose tissue, followed by entry of virus-specific T cells that resolved the infection but remained as a distinct memory cell population that expanded with obesity.[58] Upon re-challenge with LCMV, these memory T cells activated and induced necrosis in the adipose tissue of obese mice. We hypothesize that viral antigens, including CMV, in human adipose tissue could induce a similar immune response, accompanied by adverse effects on adipocyte function, with the exception that this immune response is

chronic and indolent rather than sporadic and fulminant, as in animal models of pathogen re-challenge.

An increase in specific adipose tissue immune cell subsets could be due to increased recruitment and migration from the circulation or local clonal expansion. We demonstrated that the CD69+ and CX3CR1+ CD4+ T cell subsets in adipose tissue are clonally expanded compared with CD69− CX3CR1− CD4+ T cell subsets in adipose tissue and all subsets in circulation. CX3CR1 is expressed by cytotoxic virus-specific T cells.[20,21,27,59] Furthermore, CX3CR1+ CD4+ T cells are found in tissue or blood in many autoimmune diseases, including primary sclerosing cholangitis,[60] multiple sclerosis,[61] systemic lupus erythematosus, and rheumatoid arthritis.[62,63] CX3CR1+ cells are typically CD28−, which serves as a marker of increased replicative history and oligoclonality but reduced susceptibility to apoptosis.[64–66] In contrast, CD69 has been shown to reflect tissue residency, and expression of this marker can also indicate engagement of the TCR.[33] The predominance of C-G-C+ CD4+ T cells in HIV-positive diabetics and CD69+ CD4+ T cells in HIV-negative diabetics suggests that HIV infection serves to shape the T cell profile in the adipose tissue compartment, perhaps by promoting an inflated response to specific antigens, such as CMV, and expansion of an inflammatory and apoptosis-resistant CX3CR1+ T_{EMRA} population. At present, this is speculation and further studies are needed to characterize the epitopes driving clonal proliferation of adipose tissue T cells in different disease states.

We show that adipose tissue C-G-C+ CD4+ T cells have an RNA transcriptome characterized by genes associated with leukocyte activation and cytotoxicity. We also demonstrate that adipose tissue and blood CD4+ T cells from HIV-positive persons, irrespective of diabetes status, are enriched for genes in the IL-17 differentiation pathway, as shown previously.[67,68] These cells may contribute to an adipose tissue environment high in proinflammatory cytokines that can have adverse effects on adipocyte insulin signaling and energy storage through reduced expression of several genes, such as insulin receptor substrate 1 (IRS-1), phosphatidylinositol 3-kinase (PI3K/p85α), and glucose transporter type 4 (GLUT4).[69,70] Although further human data in this area are needed, recent animal studies suggest that antigen-specific memory T cell responses in adipose tissue can contribute to adipocyte dysfunction and altered metabolic function. Mice exposed to *Yersinia pseudotuberculosis* established a population of pathogen-specific adipose tissue T cells that persisted after clearance of the initial infection. Subsequent injection with a *Y. pseudotuberculosis* peptide led to proliferation of adipose tissue memory cells and downregulation of several lipid metabolic pathways, including lipid biosynthesis and triglyceride, cholesterol, and long-chain fatty-acyl-CoA metabolic processes.[71] A similar study using LCMV, described above, reported establishment of virus-specific memory T cells in adipose tissue.[58] Upon re-challenge with LCMV, these cells expanded and induced necrosis and calcification in adipose tissue of obese mice. A study of rhesus macaques infected intrarectally with simian immunodeficiency virus (SIV; a virus similar to HIV) found detectable virus in adipose tissue stromal vascular fraction cells after acute and chronic infection.[72] Macaques chronically infected with SIV had increased adipocyte expression of peroxisome proliferator-activated receptor gamma-2

Cell Reports Medicine
Article

(PPARγ2) and decreased expression of cytosine-cytosine-adenosine-adenosine-thymidine (CCAAT)/enhancer-binding protein alpha and beta (C/EBPα and C/EBPβ, respectively), leptin, and GLUT4.

Our results propose that expansion of memory CD4$^+$ T cells in adipose tissue may contribute to alterations in adipocyte energy storage and metabolism and, ultimately, development of diabetes. This phenomenon may be exaggerated in HIV-positive persons, a group with a disproportionately high prevalence of metabolic disease, and may be driven in part by a response to the presence of viral antigens in the local environment. Further studies will determine the cognate antigens of dominant TCRs identified in adipose tissue and quantify the tissue reservoir of HIV, CMV, and other viruses in relation to immune cell populations, adipocyte energy-handling pathways, and metabolic fitness. Further studies building on our current findings may illuminate new avenues to leverage immunomodulation as a means to reduce the burden of metabolic disease, including diabetes, among persons with and without HIV.

Limitations of study

Our study has several limitations. The sample size was small, and our analysis did not include other adipose tissue immune cells, such as macrophages, dendritic cells, natural killer (NK), or NK T cells, that have been shown to interact with T cells and modulate adipocyte function. Although we identified CMV-specific T cells, our study did not quantify the burden of CMV transcripts in whole adipose tissue. Furthermore, our study used stromal vascular fraction cells obtained by small-volume fat aspiration, which limited our cell yield and was insufficient to perform *ex vivo* experiments to corroborate differential gene expression through protein expression studies. Last, our cross-sectional design precluded an assessment of causality, and future clinical studies will enroll pre-diabetic participants for longitudinal assessments to clarify the temporal relationships between the adipose tissue immune environment and metabolic health.

STAR★METHODS

Detailed methods are provided in the online version of this paper and include the following:

- KEY RESOURCES TABLE
- RESOURCE AVAILABILITY
  - Lead contact
  - Materials availability
  - Data and code availability
- EXPERIMENTAL MODEL AND SUBJECT DETAILS
  - Study population and design
  - Adipose T cell extraction and PBMC isolation
- METHOD DETAILS
  - Flow cytometry analysis
  - Bulk TCR sequencing
  - Single-cell TCR sequencing
  - 3′ and 5′ RNaseq
  - VGAS Data Analysis
  - Immunohistochemical staining
- QUANTIFICATION AND STATISTICAL ANALYSIS

REFERENCES

1. Huh, J.Y., Park, Y.J., Ham, M., and Kim, J.B. (2014). Crosstalk between adipocytes and immune cells in adipose tissue inflammation and metabolic dysregulation in obesity. Mol. Cells 37, 365–371.

2. Couturier, J., Suliburk, J.W., Brown, J.M., Luke, D.J., Agarwal, N., Yu, X., Nguyen, C., Iyer, D., Kozinetz, C.A., Overbeek, P.A., et al. (2015). Human adipose tissue as a reservoir for memory CD4+ T cells and HIV. AIDS 29, 667–674.

3. Damouche, A., Lazure, T., Avettand-Fènoël, V., Huot, N., Dejucq-Rains-ford, N., Satie, A.P., Mélard, A., David, L., Gommet, C., Ghosn, J., et al. (2015). Adipose Tissue Is a Neglected Viral Reservoir and an Inflammatory Site during Chronic HIV and SIV Infection. PLoS Pathog. 11, e1005153.

4. Damouche, A., Pourcher, G., Pourcher, V., Benoist, S., Busson, E., Latail-lade, J.J., Le Van, M., Lazure, T., Adam, J., Favier, B., et al. (2017). High proportion of PD-1-expressing CD4$^+$ T cells in adipose tissue constitutes an immunomodulatory microenvironment that may support HIV persis-tence. Eur. J. Immunol. 47, 2113–2123.

5. Couturier, J., Winchester, L.C., Suliburk, J.W., Wilkerson, G.K., Podany, A.T., Agarwal, N., Xuan Chua, C.Y., Nehete, P.N., Nehete, B.P., Grattoni, A., et al. (2018). Adipocytes impair efficacy of antiretroviral therapy. Anti-viral Res. 154, 140–148.

6. Koethe, J.R., McDonnell, W., Kennedy, A., Abana, C.O., Pilkinton, M., Setliff, I., Georgiev, I., Barnett, L., Hager, C.C., Smith, R., et al. (2018). Ad-ipose Tissue is Enriched for Activated and Late-Differentiated CD8+ T Cells and Shows Distinct CD8+ Receptor Usage, Compared With Blood in HIV-Infected Persons. J. Acquir. Immune Defic. Syndr. 77, e14–e21.

7. Wanjalla, C.N., McDonnell, W.J., Barnett, L., Simmons, J.D., Furch, B.D., Lima, M.C., Woodward, B.O., Fan, R., Fei, Y., Baker, P.G., et al. (2019). Ad-ipose Tissue in Persons With HIV Is Enriched for CD4$^+$ T Effector Memory and T Effector Memory RA$^+$ Cells, Which Show Higher CD69 Expression and CD57, CX3CR1, GPR56 Co-expression With Increasing Glucose Intolerance. Front. Immunol. 10, 408.

8. Brown, T.T., Cole, S.R., Li, X., Kingsley, L.A., Palella, F.J., Riddler, S.A., Visscher, B.R., Margolick, J.B., and Dobs, A.S. (2005). Antiretroviral ther-apy and the prevalence and incidence of diabetes mellitus in the multi-center AIDS cohort study. Arch. Intern. Med. 165, 1179–1184.

9. De Wit, S., Sabin, C.A., Weber, R., Worm, S.W., Reiss, P., Cazanave, C., El-Sadr, W., Monforte, Ad., Fontas, E., Law, M.G., et al.; Data Collection on Adverse Events of Anti-HIV Drugs (D:A:D) study (2008). Incidence and risk factors for new-onset diabetes in HIV-infected patients: the Data Collection on Adverse Events of Anti-HIV Drugs (D:A:D) study. Dia-betes Care 31, 1224–1229.

10. Capeau, J., Bouteloup, V., Katlama, C., Bastard, J.P., Guiyedi, V., Salmon-Ceron, D., Protopopescu, C., Leport, C., Raffi, F., and Chêne, G.; ANRS CO8 APROCO-COPILOTE Cohort Study Group (2012). Ten-year diabetes incidence in 1046 HIV-infected patients started on a combination antire-troviral treatment. AIDS 26, 303–314.

11. Feuerer, M., Herrero, L., Cipolletta, D., Naaz, A., Wong, J., Nayer, A., Lee, J., Goldfine, A.B., Benoist, C., Shoelson, S., and Mathis, D. (2009). Lean, but not obese, fat is enriched for a unique population of regulatory T cells that affect metabolic parameters. Nat. Med. 15, 930–939.

12. Nishimura, S., Manabe, I., Nagasaki, M., Eto, K., Yamashita, H., Ohsugi, M., Otsu, M., Hara, K., Ueki, K., Sugiura, S., et al. (2009). CD8+ effector T cells contribute to macrophage recruitment and adipose tissue inflam-mation in obesity. Nat. Med. 15, 914–920.

13. Winer, S., Chan, Y., Paltser, G., Truong, D., Tsui, H., Bahrami, J., Dorfman, R., Wang, Y., Zielenski, J., Mastronardi, F., et al. (2009). Normalization of obesity-associated insulin resistance through immunotherapy. Nat. Med. 15, 921–929.

14. Hill, D.A., Lim, H.W., Kim, Y.H., Ho, W.Y., Foong, Y.H., Nelson, V.L., Nguyen, H.C.B., Chegireddy, K., Kim, J., Habertheuer, A., et al. (2018). Distinct macrophage populations direct inflammatory versus physiological changes in adipose tissue. Proc. Natl. Acad. Sci. USA 115, E5096–E5105.

15. McDonnell, W.J., Koethe, J.R., Mallal, S.A., Pilkinton, M.A., Kirabo, A., Ameka, M.K., Cottam, M.A., Hasty, A.H., and Kennedy, A.J. (2018). High CD8 T-Cell Receptor Clonality and Altered CDR3 Properties Are Associ-ated With Elevated Isolevuglandins in Adipose Tissue During Diet-Induced Obesity. Diabetes 67, 2361–2376.

16. Tian, Y., Babor, M., Lane, J., Schulten, V., Patil, V.S., Seumois, G., Ro-sales, S.L., Fu, Z., Picarda, G., Burel, J., et al. (2017). Unique phenotypes and clonal expansions of human CD4 effector memory T cells re-express-ing CD45RA. Nat. Commun. 8, 1473.

17. Truong, K.L., Schlickeiser, S., Vogt, K., Boës, D., Stanko, K., Appelt, C., Streitz, M., Grütz, G., Stobutzki, N., Meisel, C., et al. (2019). Killer-like re-ceptors and GPR56 progressive expression defines cytokine production of human CD4$^+$ memory T cells. Nat. Commun. 10, 2263.

18. Böttcher, J.P., Beyer, M., Meissner, F., Abdullah, Z., Sander, J., Höchst, B., Eickhoff, S., Rieckmann, J.C., Russo, C., Bauer, T., et al. (2015). Func-tional classification of memory CD8(+) T cells by CX3CR1 expression. Nat. Commun. 6, 8306.

19. Nishimura, M., Umehara, H., Nakayama, T., Yoneda, O., Hieshima, K., Ka-kizaki, M., Dohmae, N., Yoshie, O., and Imai, T. (2002). Dual functions of fractalkine/CX3C ligand 1 in trafficking of perforin+/granzyme B+ cytotoxic effector lymphocytes that are defined by CX3CR1 expression. J. Immunol. 168, 6173–6180.

20. Abana, C.O., Pilkinton, M.A., Gaudieri, S., Chopra, A., McDonnell, W.J., Wanjalla, C., Barnett, L., Gangula, R., Hager, C., Jung, D.K., et al. (2017). Cytomegalovirus (CMV) Epitope-Specific CD4$^+$ T Cells Are Inflated in HIV$^+$ CMV$^+$ Subjects. J. Immunol. 199, 3187–3201.

21. Pachnio, A., Ciaurriz, M., Begum, J., Lal, N., Zuo, J., Beggs, A., and Moss, P. (2016). Cytomegalovirus Infection Leads to Development of High Fre-quencies of Cytotoxic Virus-Specific CD4+ T Cells Targeted to Vascular Endothelium. PLoS Pathog. 12, e1005832.

22. Gordon, C.L., Lee, L.N., Swadling, L., Hutchings, C., Zinser, M., Highton, A.J., Capone, S., Folgori, A., Barnes, E., and Klenerman, P. (2018). Induc-tion and Maintenance of CX3CR1-Intermediate Peripheral Memory CD8$^+$ T Cells by Persistent Viruses and Vaccines. Cell Rep. 23, 768–782.

23. Shnayder, M., Nachshon, A., Krishna, B., Poole, E., Boshkov, A., Binya-min, A., Maza, I., Sinclair, J., Schwartz, M., and Stern-Ginossar, N. (2018). Defining the Transcriptional Landscape during Cytomegalovirus Latency with Single-Cell RNA Sequencing. mBio 9, e00013-18.

24. Hotamisligil, G.S., Peraldi, P., Budavari, A., Ellis, R., White, M.F., and Spie-gelman, B.M. (1996). IRS-1-mediated inhibition of insulin receptor tyrosine kinase activity in TNF-alpha- and obesity-induced insulin resistance. Sci-ence 271, 665–668.

25. Gao, D., Madi, M., Ding, C., Fok, M., Steele, T., Ford, C., Hunter, L., and Bing, C. (2014). Interleukin-1β mediates macrophage-induced impairment of insulin signaling in human primary adipocytes. Am. J. Physiol. Endocri-nol. Metab. 307, E289–E304.

26. Lumeng, C.N., Deyoung, S.M., and Saltiel, A.R. (2007). Macrophages block insulin action in adipocytes by altering expression of signaling and glucose transport proteins. Am. J. Physiol. Endocrinol. Metab. 292, E166–E174.

27. Sacre, K., Hunt, P.W., Hsue, P.Y., Maidji, E., Martin, J.N., Deeks, S.G., Au-tran, B., and McCune, J.M. (2012). A role for cytomegalovirus-specific CD4+CX3CR1+ T cells and cytomegalovirus-induced T-cell immunopa-thology in HIV-associated atherosclerosis. AIDS 26, 805–814.

28. van de Berg, P.J., Yong, S.L., Remmerswaal, E.B., van Lier, R.A., and ten Berge, I.J. (2012). Cytomegalovirus-induced effector T cells cause endo-thelial cell damage. Clin. Vaccine Immunol. 19, 772–779.

29. Peng, Y.M., van de Garde, M.D., Cheng, K.F., Baars, P.A., Remmerswaal, E.B., van Lier, R.A., Mackay, C.R., Lin, H.H., and Hamann, J. (2011). Spe-cific expression of GPR56 by human cytotoxic lymphocytes. J. Leukoc. Biol. 90, 735–740.

30. Yue, F.Y., Cohen, J.C., Ho, M., Rahman, A.K.M.N., Liu, J., Mujib, S., Saiyed, A., Hundal, S., Khozin, A., Bonner, P., et al. (2017). HIV-Specific Granzyme B-Secreting but Not Gamma Interferon-Secreting T Cells Are Associated with Reduced Viral Reservoirs in Early HIV Infection. J. Virol. 91, e02233-16.

31. Rath, N., Wang, Z., Lu, M.M., and Morrisey, E.E. (2005). LMCD1/Dyxin is a novel transcriptional cofactor that restricts GATA6 function by inhibiting DNA binding. Mol. Cell. Biol. 25, 8864–8873.

32. Ge, S.X., Jung, D., and Yao, R. (2020). ShinyGO: a graphical enrichment tool for animals and plants. Bioinformatics 36, 2628–2629.

33. Cibrián, D., and Sánchez-Madrid, F. (2017). CD69: from activation marker to metabolic gatekeeper. Eur. J. Immunol. *47*, 946–953.

34. Kumar, B.V., Ma, W., Miron, M., Granot, T., Guyer, R.S., Carpenter, D.J., Senda, T., Sun, X., Ho, S.H., Lerner, H., et al. (2017). Human Tissue-Resident Memory T Cells Are Defined by Core Transcriptional and Functional Signatures in Lymphoid and Mucosal Sites. Cell Rep. *20*, 2921–2934.

35. Prajapati, B., Jena, P.K., Rajput, P., Purandhar, K., and Seshadri, S. (2014). Understanding and modulating the Toll like Receptors (TLRs) and NOD like Receptors (NLRs) cross talk in type 2 diabetes. Curr. Diabetes Rev. *10*, 190–200.

36. Patil, V.S., Madrigal, A., Schmiedel, B.J., Clarke, J., O'Rourke, P., de Silva, A.D., Harris, E., Peters, B., Seumois, G., Weiskopf, D., et al. (2018). Precursors of human CD4$^+$ cytotoxic T lymphocytes identified by single-cell transcriptome analysis. Sci. Immunol. *3*, 3.

37. Thome, J.J., Yudanin, N., Ohmura, Y., Kubota, M., Grinshpun, B., Sathaliyawala, T., Kato, T., Lerner, H., Shen, Y., and Farber, D.L. (2014). Spatial map of human T cell compartmentalization and maintenance over decades of life. Cell *159*, 814–828.

38. Qi, Q., Liu, Y., Cheng, Y., Glanville, J., Zhang, D., Lee, J.Y., Olshen, R.A., Weyand, C.M., Boyd, S.D., and Goronzy, J.J. (2014). Diversity and clonal selection in the human T-cell repertoire. Proc. Natl. Acad. Sci. USA *111*, 13139–13144.

39. de Jong, A., Jabbari, A., Dai, Z., Xing, L., Lee, D., Li, M.M., Duvic, M., Hordinsky, M., Norris, D.A., Price, V., et al. (2018). High-throughput T cell receptor sequencing identifies clonally expanded CD8+ T cell populations in alopecia areata. JCI Insight *3*, e121949.

40. De Neuter, N., Bartholomeus, E., Elias, G., Keersmaekers, N., Suls, A., Jansens, H., Smits, E., Hens, N., Beutels, P., Van Damme, P., et al. (2019). Memory CD4$^+$ T cell receptor repertoire data mining as a tool for identifying cytomegalovirus serostatus. Genes Immun. *20*, 255–260.

41. DeWitt, W.S., Yu, K.K.Q., Wilburn, D.B., Sherwood, A., Vignali, M., Day, C.L., Scriba, T.J., Robins, H.S., Swanson, W.J., Emerson, R.O., et al. (2018). A Diverse Lipid Antigen-Specific TCR Repertoire Is Clonally Expanded during Active Tuberculosis. J. Immunol. *201*, 888–896.

42. Emerson, R.O., DeWitt, W.S., Vignali, M., Gravley, J., Hu, J.K., Osborne, E.J., Desmarais, C., Klinger, M., Carlson, C.S., Hansen, J.A., et al. (2017). Immunosequencing identifies signatures of cytomegalovirus exposure history and HLA-mediated effects on the T cell repertoire. Nat. Genet. *49*, 659–665.

43. Gomez-Tourino, I., Kamra, Y., Baptista, R., Lorenc, A., and Peakman, M. (2017). T cell receptor β-chains display abnormal shortening and repertoire sharing in type 1 diabetes. Nat. Commun. *8*, 1792.

44. Henderson, L.A., Volpi, S., Frugoni, F., Janssen, E., Kim, S., Sundel, R.P., Dedeoglu, F., Lo, M.S., Hazen, M.M., Beth Son, M., et al. (2016). Next-Generation Sequencing Reveals Restriction and Clonotypic Expansion of Treg Cells in Juvenile Idiopathic Arthritis. Arthritis Rheumatol. *68*, 1758–1768.

45. Latorre, D., Kallweit, U., Armentani, E., Foglierini, M., Mele, F., Cassotta, A., Jovic, S., Jarrossay, D., Mathis, J., Zellini, F., et al. (2018). T cells in patients with narcolepsy target self-antigens of hypocretin neurons. Nature *562*, 63–68.

46. Lindau, P., Mukherjee, R., Gutschow, M.V., Vignali, M., Warren, E.H., Riddell, S.R., Makar, K.W., Turtle, C.J., and Robins, H.S. (2019). Cytomegalovirus Exposure in the Elderly Does Not Reduce CD8 T Cell Repertoire Diversity. J. Immunol. *202*, 476–483.

47. Rowe, J.H., Delmonte, O.M., Keles, S., Stadinski, B.D., Dobbs, A.K., Henderson, L.A., Yamazaki, Y., Allende, L.M., Bonilla, F.A., Gonzalez-Granado, L.I., et al. (2018). Patients with *CD3G* mutations reveal a role for human CD3γ in T$_{reg}$ diversity and suppressive function. Blood *131*, 2335–2344.

48. Savage, T.M., Shonts, B.A., Obradovic, A., Dewolf, S., Lau, S., Zuber, J., Simpson, M.T., Berglund, E., Fu, J., Yang, S., et al. (2018). Early expansion of donor-specific Tregs in tolerant kidney transplant recipients. JCI Insight *3*, e124086.

49. Savage, T.M., Shonts, B.A., Lau, S., Obradovic, A., Robins, H., Shaked, A., Shen, Y., and Sykes, M. (2020). Deletion of donor-reactive T cell clones after human liver transplant. Am. J. Transplant. *20*, 538–545.

50. Seay, H.R., Yusko, E., Rothweiler, S.J., Zhang, L., Posgai, A.L., Campbell-Thompson, M., Vignali, M., Emerson, R.O., Kaddis, J.S., Ko, D., et al. (2016). Tissue distribution and clonal diversity of the T and B cell repertoire in type 1 diabetes. JCI Insight *1*, e88242.

51. Werner, L., Nunberg, M.Y., Rechavi, E., Lev, A., Braun, T., Haberman, Y., Lahad, A., Shteyer, E., Schvimer, M., Somech, R., et al. (2019). Altered T cell receptor beta repertoire patterns in pediatric ulcerative colitis. Clin. Exp. Immunol. *196*, 1–11.

52. Huang, H., Sikora, M.J., Islam, S., Chowdhury, R.R., Chien, Y.H., Scriba, T.J., Davis, M.M., and Steinmetz, L.M. (2019). Select sequencing of clonally expanded CD8$^+$ T cells reveals limits to clonal expansion. Proc. Natl. Acad. Sci. USA *116*, 8995–9001.

53. Dupin, N., Buffet, M., Marcelin, A.G., Lamotte, C., Gorin, I., Ait-Arkoub, Z., Tréluyer, J.M., Bui, P., Calvez, V., and Peytavin, G. (2002). HIV and antiretroviral drug distribution in plasma and fat tissue of HIV-infected patients with lipodystrophy. AIDS *16*, 2419–2424.

54. Neyrolles, O., Hernández-Pando, R., Pietri-Rouxel, F., Fornès, P., Tailleux, L., Barrios Payán, J.A., Pivert, E., Bordat, Y., Aguilar, D., Prévost, M.C., et al. (2006). Is adipose tissue a place for Mycobacterium tuberculosis persistence? PLoS ONE *1*, e43.

55. Beigier-Bompadre, M., Montagna, G.N., Kühl, A.A., Lozza, L., Weiner, J., 3rd, Kupz, A., Vogelzang, A., Mollenkopf, H.J., Löwe, D., Bandermann, S., et al. (2017). Mycobacterium tuberculosis infection modulates adipose tissue biology. PLoS Pathog. *13*, e1006676.

56. Vangipuram, S.D., Yu, M., Tian, J., Stanhope, K.L., Pasarica, M., Havel, P.J., Heydari, A.R., and Dhurandhar, N.V. (2007). Adipogenic human adenovirus-36 reduces leptin expression and secretion and increases glucose uptake by fat cells. Int. J. Obes. *31*, 87–96.

57. Zwezdaryk, K.J., Ferris, M.B., Strong, A.L., Morris, C.A., Bunnell, B.A., Dhurandhar, N.V., Gimble, J.M., and Sullivan, D.E. (2015). Human cytomegalovirus infection of human adipose-derived stromal/stem cells restricts differentiation along the adipogenic lineage. Adipocyte *5*, 53–64.

58. Misumi, I., Starmer, J., Uchimura, T., Beck, M.A., Magnuson, T., and Whitmire, J.K. (2019). Obesity Expands a Distinct Population of T Cells in Adipose Tissue and Increases Vulnerability to Infection. Cell Rep. *27*, 514–524.e5.

59. Weiskopf, D., Bangs, D.J., Sidney, J., Kolla, R.V., De Silva, A.D., de Silva, A.M., Crotty, S., Peters, B., and Sette, A. (2015). Dengue virus infection elicits highly polarized CX3CR1+ cytotoxic CD4+ T cells associated with protective immunity. Proc. Natl. Acad. Sci. USA *112*, E4256–E4263.

60. Liaskou, E., Jeffery, L.E., Trivedi, P.J., Reynolds, G.M., Suresh, S., Bruns, T., Adams, D.H., Sansom, D.M., and Hirschfield, G.M. (2014). Loss of CD28 expression by liver-infiltrating T cells contributes to pathogenesis of primary sclerosing cholangitis. Gastroenterology *147*, 221–232.e7.

61. Broux, B., Markovic-Plese, S., Stinissen, P., and Hellings, N. (2012). Pathogenic features of CD4+CD28- T cells in immune disorders. Trends Mol. Med. *18*, 446–453.

62. Katsuyama, T., Tsokos, G.C., and Moulton, V.R. (2018). Aberrant T Cell Signaling and Subsets in Systemic Lupus Erythematosus. Front. Immunol. *9*, 1088.

63. Sawai, H., Park, Y.W., Roberson, J., Imai, T., Goronzy, J.J., and Weyand, C.M. (2005). T cell costimulation by fractalkine-expressing synoviocytes in rheumatoid arthritis. Arthritis Rheum. *52*, 1392–1401.

64. Maly, K., and Schirmer, M. (2015). The story of CD4+ CD28- T cells revisited: solved or still ongoing? J. Immunol. Res. *2015*, 348746.

65. Schmidt, D., Goronzy, J.J., and Weyand, C.M. (1996). CD4+ CD7- CD28- T cells are expanded in rheumatoid arthritis and are characterized by autoreactivity. J. Clin. Invest. *97*, 2027–2037.

66. Wagner, U., Pierer, M., Kaltenhäuser, S., Wilke, B., Seidel, W., Arnold, S., and Häntzschel, H. (2003). Clonally expanded CD4+CD28null T cells in rheumatoid arthritis use distinct combinations of T cell receptor BV and BJ elements. Eur. J. Immunol. *33*, 79–84.

67. Maek-A-Nantawat, W., Buranapraditkun, S., Klaewsongkram, J., and Ruxrungtham, K. (2007). Increased interleukin-17 production both in helper T cell subset Th17 and CD4-negative T cells in human immunodeficiency virus infection. Viral Immunol. *20*, 66–75.

68. Damsker, J.M., Hansen, A.M., and Caspi, R.R. (2010). Th1 and Th17 cells: adversaries and collaborators. Ann. N Y Acad. Sci. *1183*, 211–221.

69. Lumeng, C.N., Bodzin, J.L., and Saltiel, A.R. (2007). Obesity induces a phenotypic switch in adipose tissue macrophage polarization. J. Clin. Invest. *117*, 175–184.

70. Weisberg, S.P., McCann, D., Desai, M., Rosenbaum, M., Leibel, R.L., and Ferrante, A.W., Jr. (2003). Obesity is associated with macrophage accumulation in adipose tissue. J. Clin. Invest. *112*, 1796–1808.

71. Han, S.J., Glatman Zaretsky, A., Andrade-Oliveira, V., Collins, N., Dzutsev, A., Shaik, J., Morais da Fonseca, D., Harrison, O.J., Tamoutounour, S., Byrd, A.L., et al. (2017). White Adipose Tissue Is a Reservoir for Memory T Cells and Promotes Protective Memory Responses to Infection. Immunity *47*, 1154–1168.e6.

72. Couturier, J., Agarwal, N., Nehete, P.N., Baze, W.B., Barry, M.A., Jagannadha Sastry, K., Balasubramanyam, A., and Lewis, D.E. (2016). Infectious SIV resides in adipose tissue and induces metabolic defects in chronically infected rhesus macaques. Retrovirology *13*, 30.

73. Nicholas, K.J., Greenplate, A.R., Flaherty, D.K., Matlock, B.K., Juan, J.S., Smith, R.M., Irish, J.M., and Kalams, S.A. (2016). Multiparameter analysis of stimulated human peripheral blood mononuclear cells: A comparison of mass and fluorescence cytometry. Cytometry A *89*, 271–280.

74. Picelli, S., Faridani, O.R., Björklund, A.K., Winberg, G., Sagasser, S., and Sandberg, R. (2014). Full-length RNA-seq from single cells using Smart-seq2. Nat. Protoc. *9*, 171–181.

75. Jaitin, D.A., Kenigsberg, E., Keren-Shaul, H., Elefant, N., Paul, F., Zaretsky, I., Mildner, A., Cohen, N., Jung, S., Tanay, A., and Amit, I. (2014). Massively parallel single-cell RNA-seq for marker-free decomposition of tissues into cell types. Science *343*, 776–779.

76. Islam, S., Zeisel, A., Joost, S., La Manno, G., Zajac, P., Kasper, M., Lönnerberg, P., and Linnarsson, S. (2014). Quantitative single-cell RNA-seq with unique molecular identifiers. Nat. Methods *11*, 163–166.

77. Kivioja, T., Vähärautio, A., Karlsson, K., Bonke, M., Enge, M., Linnarsson, S., and Taipale, J. (2011). Counting absolute numbers of molecules using unique molecular identifiers. Nat. Methods *9*, 72–74.

78. Grün, D., Kester, L., and van Oudenaarden, A. (2014). Validation of noise models for single-cell transcriptomics. Nat. Methods *11*, 637–640.

79. Bolotin, D.A., Poslavsky, S., Mitrophanov, I., Shugay, M., Mamedov, I.Z., Putintseva, E.V., and Chudakov, D.M. (2015). MiXCR: software for comprehensive adaptive immunity profiling. Nat. Methods *12*, 380–381.

80. Gu, Z., Gu, L., Eils, R., Schlesner, M., and Brors, B. (2014). circlize Implements and enhances circular visualization in R. Bioinformatics *30*, 2811–2812.

81. Shugay, M., Bagaev, D.V., Turchaninova, M.A., Bolotin, D.A., Britanova, O.V., Putintseva, E.V., et al. (2015). VDJtools: Unifying Post-analysis of T Cell Receptor Repertoires. PLoS Comput. Biol. *11*, e1004503.

82. Raudvere, U., Kolberg, L., Kuzmin, I., Arak, T., Adler, P., Peterson, H., and Vilo, J. (2019). g:Profiler: a web server for functional enrichment analysis and conversions of gene lists (2019 update). Nucleic Acids Res. *47* (*W1*), W191–W198.

83. Guo, L., Akahori, H., Harari, E., Smith, S.L., Polavarapu, R., Karmali, V., Otsuka, F., Gannon, R.L., Braumann, R.E., Dickinson, M.H., et al. (2018). CD163+ macrophages promote angiogenesis and vascular permeability accompanied by inflammation in atherosclerosis. J. Clin. Invest. *128*, 1106–1124.

STAR★METHODS

KEY RESOURCES TABLE

REAGENT or RESOURCE	SOURCE	IDENTIFIER
Antibodies		
CD3-BV786 (Clone SK7)	BD Biosciences	#563800, RRID: AB_2744384
CD4-PcPCy5.5 (Clone RPA-T4)	BD Biosciences	#560650, RRID: AB_1727476
CD8-A700 (Clone PRA-T8)	BD Biosciences	#557945, RRID: AB_396953
CD57-FITC (Lot 4182924)	BD PharMingen	#555619, RRID: AB_395986
CX3CR1-PE (Clone 2A9-1)	BD Biosciences	#565796, RRID: AB_2739360
CD45RO-PECF594 (Clone UCHL1)	BD Biosciences	#562299, RRID: AB_11154398
CD14-V500 (Clone M5E2)	BD Biosciences	#561391, RRID: AB_10611856
CD19-V500 (Clone HIB19)	BD Biosciences	#561121, RRID: AB_10562391
LIVE/DEAD Fixable Aqua	ThermoFisher	L34957
CD69-APC (Clone FN50)	BD Biosciences	#560711, RRID: AB_1727507
CCR7-BV421 (Clone 150503)	BD Biosciences	#562555, RRID: AB_2728119
GPR56-PECy7 (Clone CG4)	BioLegend	#358205, RRID: AB_2562089
HLA-DR APC Cy7 (Clone G46-6)	BD Biosciences	#561358, RRID: AB_10611876
HLA-DR7: EPDVYYTSAFVFPTK (EPD) Tetramer, APC	NIH Tetramer Core	N/A
HLA-DR7: DYSNTHSTRYV (DYS), APC	NIH Tetramer Core	N/A
HLA-DR7: FRDYVDRFYKTLRAEQASQE (FRD), APC	NIH Tetramer Core	N/A
CD4 (Immunohistochemistry)	Roche	#790-4423, RRID: AB_2335982
CX3CR1 (Immunohistochemistry)	Abcam	#ab8021, RRID: AB_306203
Granzyme B (Immunohistochemistry)	LifeSpan Biosciences	#LS-B7602
Biological samples		
Peripheral Blood Mononuclear Cells (PBMCs)	Vanderbilt University Medical Center – HATIM cohort	N/A
Stromal Vascular Fraction (SVF)	Vanderbilt University Medical Center – HATIM cohort	N/A
Perivascular Adipose Tissue (Formalin Fixed Paraffin Embedded)	CVPath Institute	https://www.cvpath.org/#OurResearchCapabilitiesandFacilities
Chemicals, peptides, and recombinant proteins		
Collagenase D	Roche	1088866001
RNase inhibitor	Invitrogen	Lot 1983725
Critical commercial assays		
ImmunoSEQ hsTCRB Kit	Adaptive Biotechnologies	ISK10101
Agencourt AMPure XP	Beckman Coulter	NC9933872
KAPA Universal qPCR Library Quantification Kit	Kapa Biosystems Inc.	KK4601
NEBNext® Ultra™ II FS DNA Library Prep Kit	New England Biolabs	NEB # E6177
QIAGEN Multiplex PCR Plus Kit	QIAGEN	206152
Illumina NextSeq using a 2 × 75 paired-end chemistry kit	Illumina	20024906
Deposited data		
Raw Data	This Paper	GSE159759
GRCh38 human reference genome (Ensembl rel. 92)	Genome Reference Sequence	https://www.ncbi.nlm.nih.gov/grc/human

Continued

REAGENT or RESOURCE	SOURCE	IDENTIFIER
Oligonucleotides		
OdT Primer: 5′-5Biosg/AAG CAG TGG TAT CAA CGC AGA CAA CAC CCA GAC ATT CCA TTT TTT TTT TTT TTT TTT TTT TTT TTT TTT*V*N-3′	Integrated DNA Technologies (IDT)	Custom made
TSO:: 5′-5Biosg/AAGCAGTGGTATCAACGCAGAGTA CAXXXXXXGrGrG+G-3′	Exiqon	Custom made
cDNA Amp: AAG CAG TGG TAT CAA CGC AGA (Biotin Labeled)	IDT	Custom made
INTLINK_Top: G*CAGCGGATAACAATTTCACG GCGCGCC ACTGCAGGACGTAC*T*G*T*T	IDT	Custom made
INTLINK_Bot: A*CAGTACGTCCTGCAGTGGCG CGCCTTGACTGAGCTTTA (5′ Phosphorylated/3′ dideoxycytosine)	IDT	Custom made
1st Link_Primer: GCAGCGGATAACAATTTCACG	IDT	Custom made
2nd Link Primer: CACTGCAGGACGTACTGTT	IDT	Custom made
OdT end: AAG CAG TGG TAT CAA CGC AGA CA	IDT	Custom made
TSO end: AAG CAG TGG TAT CAA CGC AGA GT	Exiqon	Custom made
TCRA: GTCACTGGATTTAGAGTCTCTCAG	IDT	Custom made
TCRB: GAGATCTCTGCTTCTGATGGCTC	IDT	Custom made
Software and algorithms		
FlowJo software (version 10.4.1)	FlowJo LLC	https://www.flowjo.com/
Cytobank (version 6.3.1)	Cytobank	https://www.cytobank.org
Seurat	Satija et al., 2015	https://github.com/satijalab/seurat/
Visual genomics analysis studio (VGAS)	iiiD contact@iiid.com. au@IIIDPerth	https://www.iiid.com.au/software/vgas
R	R Development Core Team	https://www.r-project.org/
R Studio	N/A	https://rstudio.com/
ImmunoSEQ	Adaptive Biotechnologies	https://www.immunoseq.com/
ShinyGO v0.61	South Dakota State University Bioinformatics	http://bioinformatics.sdstate.edu/go/;[32]
g:Profiler	University of Tartu	https://biit.cs.ut.ee/gprofiler/gost
Venn Diagram Maker	VIB / UGent Bioinformatics & Evolutionary Genomics	http://bioinformatics.psb.ugent.be/webtools/Venn/
PRISM 7 and 8	Graphpad Software	N/A
BioRender	BioRender	https://biorender.com

RESOURCE AVAILABILITY

Lead contact
Further information and requests for resources and reagents should be directed to and will be fulfilled by the lead contact John R. Koethe (john.r.koethe@vumc.org).

Materials availability
This study did not generate new reagents.

Data and code availability
The gene expression data generated from this study are deposited in the NIH Gene Expression Omnibus. The accession number for the sequences reported in this paper is GenBank: GSE159759. The data analysis was performed using a custom software, VGAS, which is available upon request (contact@iiid.com.au@IIIDPerth).

EXPERIMENTAL MODEL AND SUBJECT DETAILS

Study population and design

Participants in this study were members of the HIV, Adipose tissue Immunology, and Metabolism (HATIM) cohort on long-term antiretroviral treatment enrolled from the Vanderbilt Comprehensive Care Clinic between August 2017 and June 2018. This study is registered with clinicaltrials.gov, # NCT04451980. Matched HIV-negative participants with diabetes were recruited from the Vanderbilt primary care clinic within the same time frame. Hemoglobin A1c (HbA1c) and fasting blood glucose (FBG) were used to classify participants as non-diabetic, pre-diabetic, and diabetic. All HATIM participants had sustained viral suppression (HIV-1 RNA < 50 copies/ml) for the 12 months prior to adipose tissue biopsy, no known inflammatory or rheumatologic conditions, and no immuno-modulatory medications. Participants were classified as non-diabetic (HbA1c < 5.7% and FBG < 100 mg/dL), pre-diabetic (HbA1c 5.7%–6.5% and/or FBG 100–125 mg/dL) and diabetic (HbA1c $\geq$ 6.5% and/or FBG $\geq$ 126 mg/dL or on anti-diabetic medications).[7] Blood samples were collected from the study participants after at least 8 hours of fasting and used to measure clinical laboratory values including low- and high-density lipoprotein and triglycerides. The age, gender, race and other characteristics of participants included in this study are provided in Table S1, and the experimental workflow is outlined in Figure S1A.

All subjects provided written informed consent, in accordance with the Helsinki Declaration of 1975, as revised in 2000. The study was carried out in accordance with the human experimentation ethical standards of, and approved by, the Vanderbilt Institutional Review Board.

Adipose T cell extraction and PBMC isolation

Peri-umbilical subcutaneous adipose tissue was aspirated from each subject and processed within 30 minutes of the biopsy as published.[7] In brief, we anaesthetized the skin 3cm to the right of the umbilicus using 2% lidocaine. A 2mm incision was made in the skin and we infused 40ml of sterile saline into the subcutaneous adipose tissue layer. We then used a 2.1 mm blunt, side-ported liposuction catheter (Tulip CellFriendly GEMS system Miller Harvester, Tulip Medical Products, San Diego, CA, USA) to extract viable adipocytes and stromal vascular fraction cells. The tissue was placed in approximately 50cc of cold saline. Visible clots were removed and the tissue was rinsed repeatedly with cold saline over a 70 μm mesh filter. For single cell isolation, the adipose tissue was homogenized using a gentleMACS Dissociator (Miltenyi Biotec, Bergisch Gladbach, Germany) and then incubated with collagenase (Roche Catalog #11088866001) and DNase. The adipose stromal vascular fraction was separated using a Ficoll-Paque Plus density gradient. Samples were cryopreserved in fetal bovine serum with 10% DMSO in liquid nitrogen.

Fasting blood was collected in vacutainers containing EDTA at the same time as the adipose tissue biopsy. PBMCs were separated using a Ficoll-Paque Plus density gradient. Samples were cryopreserved in fetal bovine serum with 10% DMSO in liquid nitrogen. Paired PBMC and adipose samples from each subject were thawed and run for flow cytometry and sorting on the same day.

METHOD DETAILS

Flow cytometry analysis

Matched cryopreserved PBMC and adipose tissue samples were quickly thawed in a water bath (37°C) and resuspended in 12ml of RPMI 1640 medium with 10% fetal bovine serum (FBS). Cells were centrifuged and resuspended in 12ml PBS for one more wash. Pelleted cells were resuspended in 200 μL PBS and stained on the same day with the multiple panels of fluorescently tagged antibodies (CD3, CD4, CD8, CD45RO, CCR7, CD57, CD69, GPR56, CX3CR1, HLA-DR, CD14, CD19, and LIVE/DEAD fixable aqua).[7] CX3CR1 and CCR7 stains were first performed at 37°C for 15 minutes, followed by staining with the rest of the antibodies as a master mix for 20 minutes at room temperature. We washed samples with 2ml PBS and resuspended them in 300 μL PBS with RNSase later and placed on ice until samples were sorted on the same day using a 4-laser FACSAria III cell sorter (BD Biosciences). Samples were sorted in a BSL2 laboratory and were not fixed prior to this. Single-cell sorts were performed using a 100uM nozzle into individual 96-well plates containing 4ul of phosphate buffered saline (PBS) and RNase later, bulk-sorts were performed using a 100uM nozzle into Eppendorf tubes. Sorted cells were immediately frozen on dry ice and stored at −80°C until processing below. Data analysis was performed using FlowJo software (version 10.4.1) and Cytobank (version 6.3.1).[73] UMAP embeddings were calculated with the uwot R package using default settings.

Bulk TCR sequencing

Bulk sequencing was performed using an assay to sequence the TCRβ. CD4 and CD8 T cells that had been bulk sorted into Eppendorf tubes were pelleted and resuspended in about 20ul of PBS and frozen until analysis. The cells were resuspended in 2x lysis buffer (final concentration in lysis buffer are 10mM Tris.Hcl, ph8.0, 0.1% Triton X-100, 400UG/ml Proteinase K) and incubated at 55°C for 10 hours and then 95°C for 5 minutes to inactivate proteinase K. This was performed in a programmed PCR machine. The cell lysate was used for bulk TCR sequencing immediately after lysis or stored at −20°C until use. Working dilutions of DNA samples were prepared per hsTCRβ immunoseq protocol (https://www.immunoseq.com/assays/). All possible recombined receptor sequences in a sample were amplified using a proprietary mix of multiplexed V- and J-gene primers in a first round of PCR amplification. High-throughput sequencing and unique identification of each library were made possible through the addition of universal adaptor sequences and DNA barcodes unique to each PCR replicate in a second round of PCR. Following the second PCR amplification, sequencer-ready

libraries were pooled for sequencing on an Illumina NextSeq. Data analyses including Clonality, V(D)J segments, and Morisita indices analyses were performed using the ImmunoSEQ Analyzer v3.0. We did not purify DNA for this assay to reduce chances of cross-contamination. Quality control did not show excessive sharing of TCRβ clones. One TCR that was identified as a probable contaminant was excluded from the analysis.

Single-cell TCR sequencing

The single cell RNA-sequencing (scRNA-seq) method used in this study is an adapted version of the SMARTseq2 and MARS-seq approach in which single cells from the target population are FACS-sorted into 96- or 384-well plates containing 3μL of lysis buffer inclusive of a ribo-nuclease inhibitor.[74,75] Sorted plates were stored at −80°C. The method described here is not restricted by cell size, shape or number. The assay utilized uniquely tagged primers for reverse transcription and template switching with a pre-amplification step to increase the yield and transcript length of the single cell cDNA library. During the initial reverse transcription step, cDNA was tagged with well-specific barcodes coupled with a unique molecular identifier (UMI) to allow for multiplexing and increased sample throughput. Samples were then pooled and amplified using the KAPA HiFi HotStart ReadyMix (Roche, Basel, Switzerland), as per the manufacturer's instructions. UMIs enabled quantitation of individual gene expression levels within single cells, thereby reducing technical variability and bias introduced during the amplification step.[76–78] Nested PCRs were performed to target TCR region specifically or 3′and 5′ transcriptome. See STAR methods for primer sequences.

Two microlitres of pooled cDNA was enriched for TCR alpha and beta genes using the TSOend primer and the constant region primers, TCRA or TCRB. PCR products were purified using Agencourt AMPure XP (Beckman Coulter, CA, UWA) and pooled in equimolar amounts. Indexed libraries were created for sequencing using Truseq adapters and quantified using the KAPA Universal qPCR Library Quantification Kit (Kapa Biosystems Inc., MA, USA), as per the manufacturer's instructions. Samples were sequenced on an Illumina MiSeq using a 2 × 300bp paired-end chemistry kit (Illumina Inc., CA, USA), as per the manufacturer's instructions. Reads were quality-filtered and passed through a demultiplexing tool to assign reads to individual wells and mapped to the TCRA and TCRB loci. TCR clonotypes were assigned using the MIXCR software[79] prior to analysis using the Visual genomics analysis studio (VGAS), an in-house program for visualizing and analyzing TCR data (https://www.iiid.com.au/software/vgas).

3′ and 5′ RNaseq

Up to 100ng of pooled cDNA was randomly digested and end-repaired for 30 minutes at 37°C, followed by 30 minutes at 65°C using the NEBNext® Ultra™ II FS DNA Library Prep Kit (New England Biolabs, Ipswich, MA), as per the manufacturer's instructions. The resultant short 200–400bp fragments were end-repaired, and A-tailed products were ligated with 10pmol of linker using End-repair ligation module (New England Biolabs), as per the manufacturer's instructions. After purification, products were amplified using a nested approach. Initially, products were amplified using the biotinylated primer cDNA Amp and the linker primer 1stLink_Primer (10μM). Cycling conditions were 98°C for 3 minutes, followed by 15 cycles of 98°C for 1 minute, 62°C for 30 s and 72°C for 1 minute, followed by 72°C for 10 minutes. This step allowed for the enrichment of both 5′ and 3′ ends of the cDNA fragments. After purification using Agencourt AMPure XP (Beckman Coulter), nested PCR was performed in duplicate with the same cycling conditions but for 30 cycles using either the OdTend and 2ndLink_Primer or the TSOend and 2ndLink_Primer to capture the 3′end and 5′end cDNA targets, respectively. Nested PCR was performed using the GoTaq® Hot Start Polymerase M5006 chemistry (Promega, MDN, WI), as per the manufacturer's instructions.

Purified amplicons from the 3′ and 5′ were pooled to equimolar amounts and indexed libraries were created for sequencing using Truseq adapters and quantified using the Kapa universal qPCR library quantification kit (Kapa Biosystems Inc., MA, USA). Samples were sequenced on an Illumina NextSeq using a 2 × 75 paired-end chemistry kit (Illumina Inc., CA, USA), as per the manufacturer's instructions. Reads were quality-filtered and passed through a demultiplexing tool to assign reads to individual wells and to the 3′ end and 5′ end. Reads for the individual single-cells were demultiplexed using plate-id (30 nt), and cell barcode (6 nt). The reads were further demultiplexed as either 3′ or 5′ using primer sequence (30 nt) and the remainder 45 nt sequences were aligned to the GRCh38 human reference genome (Ensembl rel. 92) using the CLC Genomics Workbench (CLC Bio) (v.11, QIAGEN Bioinformatics). An eight nucleotide UMI tag and mapping coordinates were used to remove PCR-duplicate reads. Gene-specific read counts were calculated using HTSeq-count using the latest Gencode annotations and the 3′ and 5′ counts were summed. Cells with less than 200 genes and more than 5% mitochondrial content were removed, to filter out lower quality or dying cells based on Satija lab (https://satijalab.org/seurat/v3.1/pbmc3k_tutorial.html). Furthermore, genes with > 0 counts in fewer than three cells were also removed. Downstream analyses (normalization, PCA, differential expression and visualization) were performed in Seurat v.2.3.4 R package and the VGAS program described below.

VGAS Data Analysis

VGAS is an integrative analysis program with self-standing modules that we used for single cell RNA-seq and TCR analysis (https://www.iiid.com.au/software/vgas). It is a Windows-based analysis and visualization software that is written in C sharp programming language using the .NET framework. The modules have been designed so that the end-user can query genes after quality control has removed cells that do not meet the gene threshold. For differential gene expression analysis, we uploaded metadata files and gene expression data from the 3′ and 5′ RNA sequencing in CSV format. Differential gene expression analysis was performed using the Wilcoxon rank-sum test to compare two groups or one-way ANOVA to compare more than two groups. Multiple testing correction

where indicated was performed using the Benjamini-Hochberg correction. The fold change, *p-value*s and adjusted *p-value*s are provided as supplemental data in excel sheets. TCR analysis from single-cell sequencing was performed using the TCR module in VGAS. These modules use R-tools including VDJtools and circlize.[80,81] TCR clonotypes were assigned using the MiXCR software as described above. CSV files with TCRαβ pairs assigned through MiXCR software were uploaded into VGAS to generate circos plots. We performed gene enrichment analysis using g:Profiler[82] and ShinyGO v0.61 (FDR cutoff 0.05, showing the top significant terms).[32]

Immunohistochemical staining

Human coronary artery autopsy samples with adjacent perivascular adipose tissue from an HIV-positive and an HIV-negative donor with a similar degree of atherosclerosis, and from two HIV-positive donors with and without a recorded diagnosis of diabetes prior to death, were obtained from CVPath Institute Registry for immunohistochemical staining as previously published.[83] Briefly, the artery segments were fixed in formalin, and 2 to 3 millimeter segments were embedded in paraffin. Sections of 5 microns thick were cut from each of the segments and mounted on slides. Immunohistochemistry for CD4, CX3CR1 and granzyme B were performed on the sections using Ventana DISCOVERY Ultra system (Roche). Slides were incubated with CX3CR1 antibody (Abcam ab8021, 1:1000 dilution), CD4 (Roche, 790-4423, pre-diluted) or anti-granzyme B (LifeSpan Biosciences LS-B7602) and developed by the NovaRed kit (Vector Laboratories). The images were captured by Axio Scan. Z1 (Zeiss, Germany) using a 20X objective, and images were processed and prepared on the HALO image analysis platform (Indica Labs, Corrales, NM).

QUANTIFICATION AND STATISTICAL ANALYSIS

Statistical differences between two groups were calculated using Mann-Whitney U test, and differences between paired samples using Wilcoxon signed rank test (Graphpad prism version 7 and 8). A p value < 0.05 is denoted by * in the images and considered statistically significant. Other details are included in the figure legends. Differential gene expression for the RNA transcriptome analyses were analyzed using Kruskal-Wallis test or one-way ANOVA, depending on the number of groups compared, with Benjamini Hochberg correction for multiple comparisons (Visual genomics analysis studio, VGAS). Statistical analysis is shown in supplemental Excel tables referenced in each figure. Pathway enrichment analysis was performed by applying p < 0.1 as a threshold and performed in ShinyGo based on hypergeometric distribution followed by FDR correction and g:Profiler.